EXPERIMENTAL STUDY OF WAVE INTERACTIONS WITH SLOTTED BARRIERS

BY
SUNDARALINGAM PREMASIRI

BSc.Eng(Hons), University of Peradeniya,1992
M.Eng, University of Tokyo,1995

A THESIS SUBMITTED IN PARTIAL FULFILMENT OF
THE REQUIREMENTS FOR THE DEGREE OF
MASTER OF APPLIED SCIENCE

in

THE FACULTY OF GRADUATE STUDIES
Department of Civil Engineering

We accept this thesis as conforming
to the required standard

THE UNIVERSITY OF BRITISH COLUMBIA
January 1997

In presenting this thesis in partial fulfillment of the requirements for an advance degree at the University of British Columbia, I agree that the Library shall make it freely available for reference and study. I further agree that permission for extensive copying of this thesis for scholarly purposes may be granted by the head of the department or by his or her representatives. It is understood that copying or publication of this thesis for financial gain shall not be allowed without my written permission.

Department of Civil Engineering,
The University of British Columbia,
2324 Main Mall,
Vancouver, B.C.,
Canada, V6T 1Z4

Date: Jan. 16th. 1997.

Abstract

This thesis describes an investigation of the performance of vertical single and double wave barriers. An experimental investigation of the reflection and transmission of regular and irregular waves was carried out. Measurements from three wave probes were used to analyze the reflection coefficient using a least squares method. In the tests, the wave period, wave height, barrier immersion depth, and barrier porosity were varied in order to determine the relationship between the reflection and transmission coefficients and parameters describing incident wave and barrier characteristics, such as the immersion depth, the distance between barriers and the barrier porosity. The results show that the reflection and transmission coefficients are functions of wave length, immersion depth, distance between barriers and porosity. The frequency dependent transmission coefficient obtained from irregular wave tests was compared with those obtained in regular wave tests. Single barrier and double barrier results have also been compared with predictions based on available theoretical methods. The performance characteristics of single and double barriers have been compared, and it is found that there is a significant reduction in wave transmission in the case of double barrier, without a corresponding increase in wave reflection.

Table of Contents

List of Tables

List of Figures

List of Symbols

a_i	incident wave amplitude
a_r	reflected wave amplitude
a_t	transmitted wave amplitude
A_n	Fourier coefficients
b	distance between the two barriers
d	still water depth
f_0	fundamental frequency
g	gravitational acceleration
h	immersion depth of the barrier
H	wave height
k	wave number
K_e	energy loss coefficient
K_r	reflection coefficient
K_t	transmission coefficient
$K_r(f)$	reflection coefficient as a function of frequency
$K_t(f)$	transmission coefficient as a function of frequency
L	wave length
m_0	zeroth moment of the incident wave
m_{0r}	zeroth moment of the reflected wave
m_{0t}	zeroth moment of the transmitted wave
S(f)	incident spectral density

$S_r(f)$	reflected spectral density
$S_t(f)$	transmitted spectral density
$S_\eta(f)$	spectral density of η
t	time
T_r	record length
x	horizontal coordinate in x-direction
β	phase angle between reflected waves and incident waves
δ_n	measured phase of the n^{th} wave record relative to the first
Δ_n	dimensionless distance between the n^{th} probe and first probe, $k\lambda_n$
ϕ_n	random phase angles of each component
λ_n	the distance between the n^{th} probe and the first probe
η	water surface elevation
σ_η	variance of water elevation
ω	wave angular frequency
ε	porosity of the barrier

Acknowledgments

The author would like to thank his supervisor Dr. Michael Isaacson for his guidance and encouragement throughout the preparation of this thesis. The author would like to express his gratitude to Kurt Nielson for his help in building the model and other facilities associated with the experimental investigation and to Shankar Bhat for his help relating to the experimental setup, computing and the wave generator facilities. Also, Nathalie, Sumathy and Yang are thanked for their help in running the experiments. Finally, the financial support in the form of a Research Assistantship from the Department of Civil Engineering is gratefully acknowledged.

1. Introduction

1.1 General

Engineers have devised many different kinds of structures to protect coastal activities from waves, including rubblemound breakwaters constructed of rock or concrete units, caissons filled with earth or concrete, large concrete floats, various categories of floating breakwaters, and thin barriers supported above the seabed by piling. Each of these categories of structure has its place where it can be optimally used for wave protection, depending on wave severity, water depth, costs, and environmental constraints.

In certain cases, breakwaters in the form of thin, rigid vertical barriers have been considered or adopted. A barrier which extends down from the water surface has the advantages of allowing water circulation, fish passage, and sediment transport, and addresses many other environmental concerns. In addition, such a wave barrier can also be used as a foundation system for deep water docks and for large vessels and other large floating structures. This type of breakwater has several advantages compared to conventional bottom-founded breakwaters. For instance, it is possible to attenuate incident waves without stopping steady currents, which is sometimes preferable near a river mouth or in a tidal region. In contrast to an impermeable barrier, if the barrier is permeable, waves may be transmitted through the barrier to some extent, there is an increased level of wave energy dissipation, and the resultant force acting on a permeable wave barrier may be lower than for a corresponding impermeable barrier.

A single barrier alone will typically dissipate a relatively low level of the incident wave energy, and certain arrangements of two or more barriers may be devised to increase wave energy dissipation and to yield acceptable levels of wave reflection, while restricting the extent of wave transmission.

Therefore these types of wave barrier may greatly increase the ability and flexibility to provide competent designs for coastal protection. The principal design concerns that are relevant here include reasonably low transmission of waves past the barrier, reduced wave loads acting upon the barrier, and reflected wave conditions that are not unduly severe. The goal of this study is to analyze the responses of different type of single and double wave barrier systems under a range of regular and irregular wave conditions.

1.2 Literature Review

1.2.1 Single Vertical Barrier

The effects of waves impinging on vertical thin barriers have been studied analytically by several authors. Ursell (1947) developed a theory for the partial transmission and reflection of water waves for a fixed vertical thin barrier extending from the water surface to some distance below the surface in deep water. This method involves an integral equation procedure based on Havelock's expansion of the velocity potential.

Wiegel (1960) devised an approximate solution for this case but applicable to arbitrary depths. This is based on the assumption that the transmitted wave energy flux is equal to the portion of incident wave energy flux associated with the region below the barrier. He described corresponding laboratory tests in which a barrier was subjected to waves with several wave steepness values for each of three values of relative depth. A trend of decreasing values of the transmission coefficient with increasing wave steepness was observed. The results were compared with predictions of this power transmission theory. For deep water wave conditions, the power-transmission theory was found to predict the transmission coefficient more closely than does Ursell's theory for smaller values of barrier immersion, but less well for larger values of barrier immersion.

Liu (1982) solved the related case of an inclined submerged rigid thin barrier problem using the boundary integral equation method (BIEM).

Kakuno (1983) analyzed wave reflection and transmission by an infinite array of vertical thin walls, circular cylinders, and rectangular cylinders as a boundary-value problem by applying the method of matched asymptotic expansions. A series of laboratory experiments were also carried out in order to measure reflection and transmission coefficients in a wave tank.

Memos and Christodoulou (1983) examined the behaviour of a perforated screen breakwater, with reference to its geometrical parameters and to changes in incident wave conditions. Theoretical predictions were developed on the basis of the theory of acoustics, relating to the conductivity of a hole and the resonance of a cavity. The experiments were conducted for various combinations of wave steepness, the diameter of the circular perforations and the screen width.

Hagiwara (1984) proposed a theoretical analysis using an integral equation derived for the unknown velocity component in a pervious wall for estimating the reflection and transmission coefficients of upright structures for wave dissipation. Various factors relating to wave and structural conditions were investigated. Two-dimensional experiments were conducted in order to calculate reflection and transmission coefficients and hence to provide a validation of the integral equation method.

Losada (1994) developed a solution for the case of short crested irregular waves impinging obliquely incident on a row of vertical thin barriers.

Abul-Azm (1994) developed a solution for this case based on an eigenfunction expansion method, and involving a least squares method to calculate the coefficients appearing in the eigenfunction expansion. This method gave reasonable results when compared to available experimental data. Isaacson (1996) also developed a numerical solution for this

case, based on the eigenfunction method, and used this to propose a simplified procedure for estimating wave effects on the barrier. Yu (1996) solved the corresponding problem for the case of a permeable barrier extending for seabed to the free surface.

1.2.2 Screen Type Barriers

The preceding description relates largely to single vertical barriers, a brief summary of previous work relating to screen type barriers is now given.

Marks and Jarlan (1968) carried out model tests on a perforated breakwater system which consists of a perforated front wall and a solid back wall. The elevation of the breakwater walls above the seabed was varied. Force measurements were made in three long-crested irregular wave systems. Terrett et al (1968) also conducted tests on a cellular structure having a perforated front wall and solid back wall. Measurements were made of wave reflections and wave forces.

Gardner et al. (1986) reported on model tests of a slotted vertical screen breakwater. The purpose of the tests was to measure the reflection and transmission coefficients for single and double screens, in the context of the conceptual design of a marina at Plymouth, England. Random waves were used in the tests and wave measurements were obtained using three wave probes.

Bennett et al. (1992) described a theory for calculating the reflective properties of wave screen breakwaters both with and without a solid back wall. The formulation combines linear wave theory with a semi-empirical description of eddy-shedding at the screens. A set of experiments was carried out in a wave flume in order to provide a comparison with the theoretical results. Losada et al. (1993) discussed the theoretically use of an array of permeable screens which have decreasing porosity towards a solid rear wall of a flume so as to a give a minimal level of reflection.

Yang (1996) developed a numerical model used to predict the interaction of a regular small amplitude wave train with both single and double permeable vertical barriers extending from the water surface to some distance above the seabed. His approach is based on an eigenfunction expansion method and utilizes a boundary condition at the barrier surface which accounts for energy dissipation within the barrier.

1.3 Research Objectives

Despite the considerable research conducted to date on this topic, the behaviour of such structures is still not well understood. This is due to the large number of parameters affecting breakwater performance, accounting for the wave conditions and the breakwater geometry. It is therefore necessary to study further various aspects of wave-structure interactions in the context of single and double permeable and impermeable thin vertical wave barriers.

Specially, the objectives of the present investigation are to carry out laboratory tests to assess the influence of various design parameters for the following type of wave barriers:

- single slotted barrier
- single impermeable barrier
- double slotted barrier
- double impermeable barrier

It is intended that this assessment is carried out for both regular and random waves. A limited comparison with the recent theoretical model of Yang (1996), as well as several other numerical models is also intended.

2. THEORETICAL BACKGROUND

This chapter describes the reflection of uni-directional regular and random waves. Initially, the transmitted and reflected coefficients arising from an incident wave train propagating past a barrier are developed on the basis of a linear superposition of incident and reflected waves upwave of the barrier; and a single transmitted wave train down wave of the barrier.

2.1 Regular Uni-Directional Waves

The general case of normal reflection of regular waves is considered. The free surface elevation is assumed to correspond to the superposition of sinusoidal incident and reflected wave trains. For convenience, the origin of the horizontal co-ordinate x may be defined at the intersection of the reflecting structure with the still water level as indicated in Fig. 4 The water surface elevation η in front of barrier may be expressed as

$$\eta = a_i \cos(kx - \omega t) + a_r \cos(-kx - \omega t + \beta) \tag{2.1}$$

where a_i and a_r are the amplitudes of the incident and reflected wave trains, respectively; and β is the phase angle that describes the phase of the reflected waves as the phase difference between the incident and reflected wave trains at $x = 0$ or $t = 0$. Also k and ω are the wave number and wave angular frequency respectively, and are related by the linear dispersion relation:

$$\omega^2 = gk \tanh(kd) \tag{2.2}$$

where d is the still water depth. The reflection and transmission coefficients are defined by

$$K_r = \frac{a_r}{a_i} \tag{2.3}$$

$$K_t = \frac{a_t}{a_i} \tag{2.4}$$

where a_t is the transmitted wave amplitude behind the barrier.

The energy dissipation coefficient K_e is defined as the proportion of incident wave energy flux that is dissipated by the barrier. A balance of energy flux requires that the energy flux of the incident wave train is equal to the energy flux of the transmitted and reflected wave trains, together with the energy flux that is dissipated. Since energy flux is proportional to wave height squared, this statement of energy balance can be expressed as

$$K_r^2 + K_t^2 + K_e = 1 \tag{2.5}$$

An energy conservation coefficient $K_c = 1\text{-}K_e$, which is defined as the proportion of incident wave energy flux that is conserved is also sometimes used (Sarpkaya and Isaacson, 1981).

2.2 Irregular Uni-Directional Waves

The preceding summary may be extended to the case of an irregular uni-directional wave train. An irregular signal, such as the water surface elevation due to an irregular wave train, may be assumed as periodic over a sufficiently large duration and hence may be

represented by a Fourier series which contains components at multiples of the fundamental frequency f_0. This may be written as follows:

$$\eta(t) = \sum_{n=1}^{\infty} A_n \cos(2\pi n f_0 t - \phi_n) \tag{2.6}$$

where A_n are Fourier coefficients representing the amplitudes of each individual frequency component, ϕ_n are the random phase angles of each component, and f_0 is the fundamental frequency given by $f_0 = 1/T_r$, where T_r is the record length. The variance of the signal may be written as:

$$\sigma_\eta^2 = \sum_{n=1}^{\infty} \frac{1}{2} |A_n|^2 \tag{2.7}$$

Thus $|A_n|^2/2$ represents the contribution to the variance which is associated with the frequency component nf_0. If the signal period is increased such that $f_0 \to 0$, with the signal now considered to contain a continuous range of frequencies rather than discrete harmonics, the above summation may be replaced with an integral, and the variance may then be written as:

$$\sigma_\eta^2 = \int_0^\infty S_\eta(f)\, df \tag{2.8}$$

where $S_\eta(f)$ is the spectral density of η. $S_\eta(f)df$ represents the contribution to the variance σ_η^2 due to its content within the frequency range f to $f + df$. This may be expressed symbolically as:

$$S_\eta(f)df = \sum_{f_n}^{f_n+df} \frac{1}{2}|A_n|^2 \tag{2.9}$$

From the above equation, a relationship between the Fourier amplitudes and the spectral density can be obtained:

$$A_n = \sqrt{2S_\eta(f)f_0} \tag{2.10}$$

For the case of a reflected wave field, Eq. 2.6 may be extended to describe the water surface elevation due to the superposition of incident and reflected wave trains:

$$\begin{aligned}\eta(t) &= \sum_{n=1}^{\infty} A_n \cos(2\pi n f_0 t - \phi_n) \\ &= \sum_{n=1}^{\infty} A_{in} \cos(2\pi n f_0 t - \phi_{in}) + \sum_{n=1}^{\infty} A_{rn} \cos(2\pi n f_0 t - \phi_{rn})\end{aligned} \tag{2.11}$$

By separating the time series into contributions due to incident and reflected wave trains, it is apparent that the water surface elevation may be described by incident and reflected spectral densities, $S_i(f)$ and $S_r(f)$. If the incident spectral density and reflected spectral density are known, the reflection coefficient as a function of frequency $K_r(f)$ can be found using the result given in Eq. 2.10 :

$$K_r(f) = \frac{A_r(f)}{A_i(f)} \tag{2.12}$$

$$= \sqrt{\frac{S_r(f)}{S(f)}} \tag{2.13}$$

In the similar way, the transmission coefficient as a function of frequency $K_t(f)$ may be written as

$$K_t(f) = \frac{A_t(f)}{A_i(f)} = \sqrt{\frac{S_t(f)}{S(f)}} \tag{2.14}$$

In addition, an average reflection coefficient $\overline{K}_r$ and an average transmission coefficient $\overline{K}_t$ can be defined as follows:

$$\overline{K}_r = \left[\frac{\int_0^\infty S_r(f)\,df}{\int_0^\infty S(f)\,df} \right]^{1/2} \tag{2.15}$$

$$\overline{K}_t = \left[\frac{\int_0^\infty S_t(f)\,df}{\int_0^\infty S(f)\,df} \right]^{1/2} \tag{2.16}$$

The above formulae may be expressed clearly in terms of the zeroth moments of the corresponding spectra or the significant wave heights associated with the incident, reflected and transmitted wave trains. Thus

$$\overline{K}_r = \sqrt{\frac{m_{0r}}{m_0}} = \frac{H_{sr}}{H_s} \tag{2.17}$$

$$\overline{K}_t = \sqrt{\frac{m_{0t}}{m_0}} = \frac{H_{st}}{H_s} \tag{2.18}$$

where m_0 is the zeroth moment defined as:

$$m_0 = \int_0^\infty S(f)df \tag{2.19}$$

and the significant wave height is related to the zeroth moment by:

$$H_s = 4\sqrt{m_0} \tag{2.20}$$

The subscripts r and t refer to the reflected and transmitted wave trains repectively; otherwise the incident wave train is implied.

2.3 Dimensional Analysis

In planning the model tests and the presentation of results, it is useful to carry out a dimensional analysis of the problem in order to identify the governing parameters so that controlled variables in the model can be suitably varied.

A rigid wave barrier extending to a depth h below the still water level is subjected to a uni-directional, regular, nonbreaking wave train propagating normally to the barrier (Fig. 1). There are a number of dependent variables which are indicative of barrier performance and which are used in design. These include the reflected wave height, the transmitted wave height, the runup and the wave loads. However, of these only the reflected and transmitted wave heights are considered in this thesis. On the basis of a

dimensional analysis, the reflection coefficient K_r and transmission coefficient K_t may be expressed in the form:

$$K_r = f_1\left(\frac{h}{d}, kh, \frac{H}{L}, \varepsilon\right) \tag{2.21}$$

$$K_t = f_2\left(\frac{h}{d}, kh, \frac{H}{L}, \varepsilon\right) \tag{2.22}$$

where H is the wave height, L is the wave length, d is the water depth, h is the immersed depth of the barrier, and ε is the porosity of the barrier. The porosity ε is defined as the ratio of the area of gaps in the barrier face to the total area of the barrier face.

For the case of double barrier, the spacing b between the two barriers is also relevant (see Fig. 2), so that the above non-dimensional equations can be extended to:

$$K_r = f_1\left(\frac{h}{d}, kh, \frac{H}{L}, kb, \varepsilon\right) \tag{2.23}$$

$$K_t = f_2\left(\frac{h}{d}, kh, \frac{H}{L}, kb, \varepsilon\right) \tag{2.24}$$

3. Experimental Investigation

3.1 Introduction

Small scale physical models of coastal structures or structural components are a convenient means of predicting full-scale performance. The use of such models can result in considerable economies by helping to avoid disastrous mistakes in prototype design. Model tests are particularly invaluable when analytical methods of prediction are inadequate or unavailable, as in some separated flow and dynamic response problems within the general area of fluid-structure interaction. Such model tests relating to the problem at hand have been carried out in the wave flume of the Hydraulics Laboratory of the Department of Civil Engineering, University of British Columbia, Canada. The following sections describe the equipment and methods used in the experimental set-up for wave generation and data acquisition. The techniques of signal conditioning and data analysis used to derive pertinent information from measurements are also discussed.

3.2 Barrier Models

Four type of wave barrier models were constructed:

- single slotted wave barrier
- single impermeable wave barrier
- double slotted wave barrier
- double impermeable wave barrier

A full depth vertical wave barrier was constructed of perplex glass elements, each with a width of 2 cm and a thickness of 1.3 cm. The permeability of the barrier can be varied by changing the gap between each element. Five gap spacings were used with 0.1, 0.2, 0.5,

0.9, 1.4 and 2.1 cm. These values corresponds to porosities of 5%, 10%, 20%, 30%, 40% and 50% respectively. The permeable and impermeable barriers were designed to be easily raised and lowered for tests at particular depths of barrier immersion. It was mounted vertically using a steel bar as shown in Fig. 5. The steel bar can move along vertically so that the barrier immersion depths can be changed. The double wave barrier was designed such that the distance between two barriers can be changed. The model wave barrier was set up approximately 10 m downstream from paddle. Figure 6 shows the double wave barrier mounted in the wave flume. The distance b between the two barriers was set at 0.2, 0.5 and 1.0 m. The barrier was fixed with both side of the flume wall in order to prevent any motions of the barrier due to wave forces.

3.3 Wave Flume and Generator

A sketch of the Hydraulics Laboratory wave flume is shown in Fig. 3. The flume is 20 m long with a 15 m long test section, 0.62 m wide, and operates at a nominal depth of 0.55 m. An artificial beach which is covered by a mat of synthetic hair is located at the downwave end of the flume in order to minimize wave reflection. Waves are generated by a single paddle wave actuator located at the upwave end. The generator is controlled by a DEC VAX station-3200 minicomputer using the GEDAP software package developed by the National Research Council, Canada (NRC). The generator is capable of producing wave heights up to 30 cm and wave periods as low as 0.5 sec.

3.4 Control and Data Acquisition

The GEDAP general purpose software package was used extensively during all stages of the experimental investigation. This software package is available for the analysis and management of laboratory data, including real-time experimental control and data-acquisition functions. GEDAP is a fully integrated, modular system which is linked together by a common data file structure. GEDAP maintains a standard data file format

so that any GEDAP program is able to process data generated by any other GEDAP program. This package also includes an extensive set of data analysis programs so that most laboratory projects can be handled with little or no project-specific programming. An attractive feature is a fully-integrated interactive graphics capability, such that results can be conveniently examined at any stage of the data analysis process. It also includes an extensive collection of utility packages, which consist of a data manipulation routine, a frequency domain analysis routine, and statistical and time-domain analysis routines. In particular, the program RTC_SIG generates the control signal necessary to drive the wave generator, and the routine RTC_DAS reads the data acquisition unit channels and stores the information in GEDAP binary format compatible with other GEDAP utility programs.

A program RWREP2 computes the wave machine control signal for a regular wave train corresponding to a wave height and period specified by the user. The control signal file produced by program RWREP2 is sent to the wave machine controller through a D/A output channel by using the real-time control program RTC.

The software package RTC (Real Time Control) was used in all stages of the experimental procedure. RTC consists of a main hardware execution program and a command entry program that allows the user complete control over data acquisition, control loops and signal generation.

Wave generation was carried out by first loading the control signal file into RTC buffer file and then enabling the buffer to start the wave machine. When the enable command was given, the output signal was smoothly ramped up from zero amplitude to full amplitude over a period of 10 sec. This automatic ramping was carried out in order to protect the wave machine from being subjected to sudden transients in its control signal.

The program RTC was also used to measure the wave train produced by the wave machine. The wave probes were sampled at a rate of 20 kHz for a duration of 14 secs. The resulting data file was demultiplexed by running the programs PDMULT2 before the

measured wave train could be analyzed. This program is used to demultiplex a GEDAP Primary Data File (.PDF) produced by the GEDAP Data Acquisition System. The demultiplexing produces individual GEDAP compatible data files that may then be analyzed by existing GEDAP programs.

3.5 Irregular Wave Generation

Random waves can be generated either from a target spectrum based on a theoretical parametric model (e.g. the Bretschneider or JONSWAP spectra.) or from a prototype spectrum obtained from either a wave hindcasting procedure or from full-scale measurements at sea. A program PARSPEC computes the spectrum for a particular type of spectrum corresponding to a peak frequency and significant wave height specified by the user. A program RWSYN syntheses the given wave spectrum into a time series. Then the program RWREP2 computes wave machine control signal for a irregular wave train corresponding to a given time series of data.

3.6 Measurements

The wave probes used are based on a design of the Hydraulics Laboratory of the National Research Council, Canada. It is a capacitance-type 'bow-string' sensor consisting of a loop of wire stretched on one side of a metal frame. The wire loop sensor is connected to an amplifier designed to convert the change of capacitance to a measurable change in voltage. This device has a linearity better than 98.5% and a resolution better than 1 mm, the latter being limited mainly by meniscus, and under wave action, by the run-up. Three probes were used on the upwave side of the barrier at distances of 1.0 m, 1.2 m and 1.5 m from barrier and two probes were used on the downwave side at distances of 1.0 m and 1.2 m from the barrier. These probe locations were selected by considering the evanescent wave modes from the barrier, the wave paddle and the method of reflection analysis (Isaacson, 1991).

3.7 Test Program

It was expected that the wave parameters that would have the greatest influence on the reflection and transmission characteristics would be the wave length L, the wave height H, and the barrier immersion depth h. The water depth was held at a constant value d = 0.45 m for all tests, and the wave period, the wave height, the barrier immersion and the distance between barriers were varied. Table 1 lists the wave conditions used in the tests, and Tables 2 and 3 list the test programs adopted for the single and double barrier cases, respectively. Tests A1 to A5 correspond to waves with constant steepness, H/L = 0.07, and varying wave period ranging from 0.6 sec to 1.4 sec. These waves are used to examine the effects of wave periods on the barrier. Test waves B1 to B5 were used to examine the effects of wave steepness for two fixed values of wave period.

For the single barrier, the relative draft h/d was varied as shown in Table 2 in order to examine the effects of relative draft. These tests were conducted for five porosities: 5%, 10%, 20%, 30%, 40% and 50%. For the double barrier, both the relative draft h/d and relative distance between barriers b/h were varied as shown in Table 3. These tests were conducted for two porosities: 5% and 10%.

Test R1 in Table 2 represents a test carried out with a single irregular, uni-directional wave train. These tests were undertaken in order to examine how adequately the results obtained from the regular wave experiments described the characteristics of irregular wave reflection. Irregular wave train was approximately described by a Bretschneider spectrum given by

$$S_\eta(f) = \frac{5H_s^2}{16f_p}\frac{1}{\left(f/f_0\right)^5}\exp\left\{-\frac{5}{4}\left(\frac{f}{f_0}\right)^{-4}\right\} \tag{3.1}$$

where H_s is the significant wave height and f_0 is the peak frequency of the spectrum. The characteristics of the irregular waves were chosen so as to allow comparisons to be made between irregular wave results and from selected regular wave tests.

3.8 Analysis

3.8.1 Regular Uni-directional Reflection Analysis

Several methods may be used to compute the reflection coefficient from measured regular wave data. This may involve a single wave probe which is traversed along the wave direction in order to obtain the maximum and minimum wave heights; or two or more fixed probes which measure wave heights and possibly phases at the probe locations.

Various researchers such as Mansard and Funke (1980) and Isaacson (1991) have described the use of three probes applied to a least squares method. Isaacson compared several methods and found that the least squares method is generally suitable. This approach has been adopted here, and is now summarized.

3.8.2 Least Squares Method

An outline of the least squares method applied to the data for three probes is given here. The free surface elevation is assumed to correspond to the superposition of sinusoidal incident and reflected wave trains. For convenience, the origin of the horizontal coordinate x may be defined at the intersection of the reflecting structure with the still water level (Fig. 4). Time t is taken to be zero when an incident wave crest crosses $x = 0$, so that free surface elevation η may be expressed as:

$$\eta = a_i \cos(kx - \omega t) + a_r \cos(-kx - \omega t + \beta) \qquad (3.2)$$

where a_i and a_r are the amplitudes of the incident and reflected wave trains, respectively; and β is a phase angle that describes the phase of reflected waves by counting for the phase difference between incident and reflected wave trains at $x = 0$ or $t = 0$. k and ω are

the wave number and wave angular frequency, respectively and are related by the linear dispersion relationship:

$$\omega^2 = gk\tanh(kd) \tag{3.3}$$

where d is the still water depth; and g is the gravitational constant. The incident wave height H and reflection coefficient K_r are given in terms of a_i and a_r as:

$$H = 2a_i \tag{3.4}$$

$$K_r = \frac{a_r}{a_i} \tag{3.5}$$

Equation 3.2 is to be applied at a series of probe locations x_n, n = 1, 2, ... (see Fig. 4) that may be written in terms of the location of the first probe x_1 and the intervals between probes:

$$x_n = x_1 + \lambda_n \tag{3.6}$$

where $\lambda_n (n \geq 2)$ is the distance between the n-th probe and the first probe; and $\lambda_1 = 0$. This may be written as:

$$kx_n = kx_1 + \Delta_n \tag{3.7}$$

where $\Delta_n = k\lambda_n$ is the dimensionless distance between the n-th probe and the first probe; and $\Delta_1 = 0$. Equation 3.2 applied at each probe location may thus be written as:

$$\eta_n = a_i \cos(kx_n - \omega t) + a_r \cos(kx_n + \omega t - \beta) \tag{3.8}$$

$$= a_i \cos(kx_1 + \Delta_n - \omega t) + a_r \cos(kx_1 + \Delta_n + \omega t - \beta) \tag{3.9}$$

The actual measurements at the probe locations will provide corresponding amplitudes and relative phases, such that the measured elevation at the n-th probe may be written as:

$$\eta_n^{(m)} = A_n \cos(\omega t - \phi_n) \tag{3.10}$$

$$= A_n \cos(\omega t - \phi_1 - \delta_n) \tag{3.11}$$

where A_n is the measured amplitude of the water surface at the n-th probe, ϕ_1 is the absolute phase of the first probe which need not be measured, and δ_n is the measured phase of the n-th wave record relative to the first, so that $\delta_n = \phi_n - \phi_1$.

It is also useful to describe the free surface elevation in complex notation in order to simplify the algebra, with the real parts of complex expressions corresponding to the physical quantity described. Equation 3.8, expressing the elevation in terms of incident and reflected wave parameters, may be written in complex form as:

$$\eta_n = \left\{ a_i \exp(ikx_n) + a_r \exp\left[-i(kx_n - \beta)\right] \right\} \exp(-i\omega t) \tag{3.12}$$

$$= \left\{ a_i \exp\left[i(kx_1 + \Delta_n)\right] + a_r \exp\left[-i(kx_1 + \Delta_n - \beta)\right] \right\} \exp(-i\omega t) \tag{3.13}$$

The measured water elevation may be written in complex form as:

$$\eta_n^{(m)} = A_n \exp\left[i(\phi_1 + \delta_n)\right] \exp(-i\omega t) \tag{3.14}$$

The Eqs. 3.13 and 3.14 can be written as

$$\eta_n = \left[b_i \exp(i\Delta_n) + b_r \exp(-i\Delta_n)\right] \exp(-i\omega t) \quad \ldots\ldots\ldots (n = 1,2,3) \tag{3.15}$$

$$\eta_n^{(m)} = B_n \exp(-i\omega t) \tag{3.16}$$

where

$$b_i = a_i \exp(ikx_1) \tag{3.17}$$

$$b_r = a_r \exp[-i(kx_1 - \beta)] \tag{3.18}$$

$$B_n = A_n \exp[i(\phi_1 + \delta_n)] \tag{3.19}$$

The sum of the squares of the error between the complex amplitudes of the assumed and measured elevations may be written from Eqs. 3.15 and 3.16 as:

$$E^2 = \sum_{n=1}^{3} \left[b_i \exp(i\Delta_n) + b_r \exp(-i\Delta_n) - B_n\right]^2 \tag{3.20}$$

This error of fit is minimized with respect to the required complex unknowns b_i and b_r by setting $\partial E^2/\partial b_i$ and $\partial E^2/\partial b_r$ in turn to zero. This gives rise to two complex equations for b_i and b_r :

$$\sum_{n=1}^{3} \exp(i\Delta_n) \left[b_i \exp(i\Delta_n) + b_r \exp(-i\Delta_n) - B_n\right] = 0 \tag{3.21}$$

$$\sum_{n=1}^{3} \exp(-i\Delta_n)\left[b_i \exp(i\Delta_n) + b_r \exp(-i\Delta_n) - B_n\right] = 0 \tag{3.22}$$

Solving these two equations provides b_i and b_r in terms of B_n and thereby provides a_i and a_r and β in terms of A_n. This solution was expressed by Isaacson (1991) as:

$$a_i = |X_i| \tag{3.23}$$

$$a_r = |X_r| \tag{3.24}$$

$$\chi = \mathrm{Arg}(X_i) - \mathrm{Arg}(X_r) \tag{3.25}$$

where

$$X_i = \frac{s_2 s_3 - 3s_4}{s_5} \tag{3.26}$$

$$X_r = \frac{s_1 s_3 - 3s_3}{s_5} \tag{3.27}$$

and

$$s_l = \sum_{n=1}^{3} \exp(i2\Delta_n) \tag{3.28}$$

$$s_2 = \sum_{n=1}^{3} \exp(-i2\Delta_n) \tag{3.29}$$

$$s_3 = \sum_{n=1}^{3} A_n \exp[i(\delta_n + \Delta_n)] \tag{3.30}$$

$$s_4 = \sum_{n=1}^{3} A_n \exp[i(\delta_n - \Delta_n)] \tag{3.31}$$

$$s_5 = s_1 s_2 - 9 \tag{3.32}$$

3.9 Transmission Coefficient

The signals from the two probes on the downwave side were used to calculate the transmission coefficient. The transmission coefficients were calculated as ratio of the average wave height from the two probes to the incident wave height.

3.10 Irregular Wave Analysis

Analysis of the irregular wave tests required that the spectral density of the incident, reflected and transmitted wave trains be obtained. The spectral density was calculated using the GEDAP program VSD. The transmission coefficients as functions of frequency were calculated by dividing the transmitted spectral density function by the incident spectral density function as described by Eq. 3.1.

VSD is a general purpose program which uses a Fourier analysis technique to calculate the spectral density of a signal. The Fourier transform is taken and the periodogram resulting from this operation is smoothed using a simple moving average filter band

width or a specified number of degrees of freedom per spectral estimate. Output from the VSD consists of the spectral density function as well as many spectral parameters including the peak frequency and the zeroth moment of the spectrum.

4. Results and Discussion

The results of the experiments which have been described are presented and discussed in this chapter. The first section focuses on the quality of the signals that have been recorded. In the subsequent sections, results from both the single and double barrier experiments are presented and compared with selected theoretical results.

As indicated in Chapter 2, the results indicating breakwater performance relate to the wave reflection, transmission and energy dissipation coefficients and these three dimensionless parameters are considered here. Other parameters important in design, including wave runup and wave loads have not been treated.

4.1 Time Histories

Before placing the breakwater in the flume, the entire set of test wave conditions were reproduced in order to examine the incident wave field in the absence of any reflections from the barrier. This showed that the incident wave profiles were of satisfactory quality. The incident wave heights were measured and checked against those specified. During these test runs without the barrier in place, the wave probes were located in the identical positions as when the breakwater is in place.

A sample of the measured water surface elevation signal is given in Fig. 7, which shows signals from tests with and without the barrier in place. This figure shows that the combined incident and reflected wave signal is cyclic with the same frequency as the incident wave signal. No other frequencies are present in the reflected signal confirming the assumption that there is no scattering of frequency in the reflection process.

The regular wave analysis was carried out using measurements of an initial portion of the record, before undesired wave energy reflected by the beach reached the wave probes.

These precautions are taken to avoid possible errors in the results. Figure 8 shows the wave signal record at each probe position for 14 sec and the portion of record considered for the calculation of reflection coefficients. The figure indicates how the wave records at probes 1, 2 and 3, on the upwave side of the structure, are adjusted as waves reflected from the structure become established; whereas the records at probes 4 and 5, on the downwave side of the structure, remain regular since reflections from the beach do not reach the probes within the duration shown.

4.2 Single Barrier-Regular Waves

Tests have been conducted for non-breaking regular and irregular waves with a vertical barrier at two different immersion depths. As already indicated, the water elevation was measured with the structure in place at three different locations on the upwave side and at two different locations on the downwave side. The surface elevation was also measured at all five locations without the structure in place. The data has been analyzed to obtain the reflection, transmission and energy dissipation coefficients.

Typical experimental results of reflection, transmission and energy dissipation coefficients are shown as function of kh in Figs. 9 and 10 for h/d = 1.0 and 0.5 respectively.

Figures 9(a) and 10(a) show the variation of the reflection coefficient with respect to kh for various values of porosity and for two different barrier immersion depths. From these figures its apparent that the reflection coefficient K_r generally increases with kh as expected. The reflection coefficient varies from 0.1 to 0.9 for both relative drafts h/d = 0.5 and 1.0. The maximum reflection coefficient for the relative draft h/d = 1.0 and a porosity of 5% was found to be 0.9 and decreases with increasing porosity.

Figures 9(b) and 10(b) show the variation of the transmission coefficient with respect to kh for various values of porosity and for two different barrier immersion depths. As expected, the transmission coefficients is seen to have an inverse relation to the reflection coefficient. The transmission coefficient ranges from 0.3 to 0.7 for a relative draft of h/d

= 1.0 and has a minimum value of 0.3 with a porosity of 5%. For a relative draft h/d = 0.5, the transmission coefficient ranges from 0.1 to 0.9 and has a minimum value of 0.1 for an impermeable barrier.

The energy dissipation coefficient was calculated from Eq. 2.5 using the measured values of the reflection and transmission coefficients. It can be observed from Figs. 9(c) and 10(c) that the energy dissipation coefficient varies from 0.1 to 0.6.

Figure 11 shows the variation of reflection, transmission, and dissipation coefficients with wave steepness for the case of a relative draft h/d = 1.0 and for kh = 1.9. The trend of decreasing values of transmission coefficient with increasing wave steepness can be seen from this figure. This is expected, since for all other conditions being equal, the water particle velocity increases as the wave steepness increases, and thus energy loss associated with flow separation at the bottom of the barrier is expected to increase with increasing wave steepness, resulting in a decrease in the transmission coefficient.

Figures 12 and 13 show the reflection, transmission, and dissipation coefficient variations with porosity for a relative draft h/d = 1.0 and kh = 1.42, and for a relative draft h/d = 0.5 and kh = 2.5 respectively. It is apparent from the figures that, as porosity is increased, the reflection coefficient decreases, the transmission coefficient increases and the dissipation coefficient decreases.

4.3 Comparison with Analytical Results

Figure 14 shows a comparison of experimental results with the Wiegel's (1960) power theory and Isaacson's (1996) exact solution for an impermeable barrier with a relative draft h/d = 0.5. Wiegel's simplified approach predicts the transmission coefficient to be given as:

$$K_t = \sqrt{\frac{2kh + \sinh(2kh)}{2kd + \sinh(2kd)}} \tag{4.1}$$

Isaacson's simplified formula for the transmission coefficient is given as:

$$K_t = \sec h^m\left[(kh)^n\right] \tag{4.2}$$

and he proposed values of m and n as functions of h/d. For the present case h/d = 0.5, the values of m and n are 2.25 and 1.90 respectively. Isaacson's solutions are in reasonable agreement with the experimental results and follow the trend of experimental results.

Figures 15 and 16 show a comparison of the experimental results with Yang's (1996) numerical solution for a porosity 5% and relative drafts of h/d = 1.0 and 0.5 respectively; Fig. 17 shows a comparison of the experimental results with Yang (1996) and Kakuno (1983) for a relative draft h/d = 1.0 and a porosity 20%; Fig. 18 shows a comparison with Yang (1996) for h/d = 0.5 and a porosity of 20%; and Fig. 19 shows the comparison with Kakuno's predictions for h/d = 1.0 and a porosity of 50%. It can be seen from the comparisons that Yang's solution generally provides good agreement with the experimental results, but Kakuno's results only are in reasonable agreement with the experimental results for the case of a porosity of 50%. This can be explained on account of Kakuno's solution not incorporating energy losses in the system. When the porosity increases, energy losses decrease so that Kakuno's solution then provides more reasonable agreement with the experimental results.

In order to apply Yang's numerical model, suitable values of friction and added mass coefficients are needed. These are in general not known and in the present study have been estimated so as to provide a best fit between the measured and predicted values of the transmission, reflection, and energy dissipation coefficients. This procedure gives a friction coefficient of 2.0 and an added mass coefficient of 2.0 which compares favourably with the value of friction coefficient used by Yu (1995) and the value of added mass coefficient used by Hagiwara (1984) for breakwaters extending down to the seabed.

Differences between the numerical model predictions and experimental data points could be attributed to the assumptions considered in the model, which include monochromatic waves, linear wave theory and the potential flow, which does not account for the flow separation around such a sharp edged structure.

4.4 Single Barrier-Irregular Waves

The purpose of testing with irregular waves is to determine whether the results obtained from the regular wave tests are applicable in the case of irregular waves. This has been carried out by estimating spectral density functions for both incident and transmitted wave trains and thereby calculating the transmission coefficient as a function of frequency. This transmission coefficient can be directly compared to the corresponding values at each wave frequency measured in the regular wave tests.

Figures 20 and 21 show estimates of the wave spectral densities for a peak period T_p = 0.6 sec and significant wave height H_s = 0.05 m. It can be seen that the transmitted wave energy covers approximately the same frequency range as the incident wave energy. In the case h/d = 1.0 and ε = 10%, the peak frequency of the transmitted spectral density appears to be lower than that of the incident spectral density. Also, for a relative draft of h/d = 0.5 the transmitted wave spectra show relatively high amounts of transmitted wave energy over the high frequency range, f > 2.0 Hz.

Figures 22 and 23 show the transmission coefficients as function of frequency deriving from the data used for Figs. 20 and 21. These figures show that the estimated transmission coefficient for the irregular wave tests exhibit a reasonably close agreement with those measured in the regular wave tests.

4.5 Double Barrier

Tests have also been conducted with a double vertical barrier subjected to non-breaking regular waves for three different distances between the two barriers, two different immersion depths, and various porosities. The water surface elevation was measured as for the single barrier tests. Figures 24 to 32 show the corresponding results.

The reflection coefficient for a relative draft of h/d = 0.5 and various relative distances between barriers is shown in Figs. 24(a), 25(a) and 26(a) for porosities of 0%, 5% and 10% respectively. In all cases, it can be seen that the reflection coefficient increases with kh. Figures 27(a) and 28(a) show the reflection coefficient variation with kh for a relative draft of h/d = 1.0 and porosities of 5% and 10% respectively. As in the previous case, reflection increases with kh. Figures 29(a) and 30(a) show the variation of reflection coefficient with kh for the relative draft of h/d = 0.5 and relative distance b/h = 2.2 and 4.4 respectively for various porosities. The reflection coefficient does not vary very much with barrier distance for kh < 0.75 for h/d = 0.5 and kh < 1.5 for h/d = 1.0. The reflection coefficient increases with b/h when kh > 0.75 for h/d = 0.5 and kh > 1.5 for h/d = 1.0.

Figures 24(b), 25(b) and 26(b) show the transmission coefficient variation with kh for the relative draft h/d = 0.5 and for porosities 0%, 5% and 10%. Figures 29(b) and 30(b) show the variation of the transmission coefficient with kh for the porosities 5% and 10% for the different relative distances for a relative draft h/d = 0.5. It can be observed that the transmission coefficient decreases with kh. The trend observed is that the transmission coefficient is smaller for shorter waves, and decreases with porosity.

Figures 24(c), 25(c) and 26(c) show the energy dissipation coefficient variation with kh for a relative draft of h/d = 0.5 and porosities of 0%, 5% and 10%, and Figs. 27(c) and 28(c) show the variation of the energy dissipation with kh for a relative draft of h/d = 1.0 and porosities of 5% and 10%.

Figures 33 to 37 show the comparison of the performance of the single and double barriers. It can be observed from the results that the energy dissipation is generally higher than that of a single barrier. Generally the reflection coefficient does not change much between single and double barrier, but there is significant reduction in the transmission coefficient for the double barrier. In almost all the cases, the transmission coefficient reduction was found to be more than 50%. This can be explained by the greater level of energy dissipation for the double barrier than for the single barrier.

Figures 38 to 40 show comparisons of the experimental results with numerical results based on the numerical model described by Yang (1996). The comparisons are shown for a relative draft h/d = 0.5, a porosity of 5%, and for three relative spacing values: b/h = 0.9, 2.2 and 4.4. The value of the permeability parameter, which is required in the numerical model, is equal to that selected for a single barrier with the porosity of 5%. It can be observed that there is reasonable agreement between the experimental results and numerical predictions based on Yang's model. In some cases, especially for longer waves, the numerical results deviate from the experimental results. It can be seen from the results that resonance occurs in the case of double barrier. This occurrence depends on the dimensionless barrier distance kb, and mostly take place for $kb = n\pi/2$, for n = 1, 2, 3, ... Further studies are needed to verify whether this phenomenon is dependent on other parameters.

4.6 Design Considerations

It is of interest to consider the implications of the foregoing results on breakwater design and to illustrate that for a particular example. Reflection of waves into navigational channels constitutes a particular hazard to vessels, and waves reflected within harbours can significantly worsen mooring conditions. These kind of problems can be reduced by use of permeable barriers as discussed in this thesis. Thus, such barriers can be used in the design of new harbours and marinas, and the redevelopment of existing harbours. The performance of existing structures may also be improved through appropriate

modifications. Permeable vertical barriers can be constructed by forming closely spaced elements such as steel or timber piles, concrete or timber planks, or other pre-cast concrete elements. The screen elements can be supported by steel or timber piles. The following example describes a design problem.

Cases considered correspond to both a single barrier and a double barrier, and with porosities of both 0% and 10%. The barriers are located in a water depth d = 8m, they have a draft h = 4 m, and are subjected to wave conditions corresponding to a wave period T = 4 sec and wave height H = 1.2 m. The spacing of the double barrier is taken as b = 9 m. The relative draft is thus h/d = 0.5 and the relative spacing is b/h = 2.3. On the basis of linear dispersion relation, the governing parameters kh, h/d, and b/h are 1.039, 0.50 and 2.3 respectively.

On the basis of Fig. 10, for the single barrier, the transmitted wave height is calculated as 0.48 m and 0.72 m for porosities of 0% and 10% respectively, while the reflected wave height is calculated as 0.78 m and 0.51 m for porosities of 0% and 10% respectively. From Figs. 24 and 26, for the double barrier, the transmitted wave height is calculated as 0.12 m and 0.46 m for porosities of 0% and 10% respectively and the reflected wave height is calculated as 0.65 m and 0.55 m for porosities of 0% and 10% respectively.

It can be seen notably for this case, that the reflected wave height for a single permeable barrier is less than that of an impermeable barrier, while the transmitted wave height increases to a corresponding extent. As expected the double permeable barrier gives better results than the single permeable barrier in terms of both the reflected and transmitted wave heights. Either a single permeable barrier or double barrier can be used depending on the design requirements.

5. Conclusions and Recommendations

This thesis describes an investigation of the performance of vertical single and double permeable wave barriers. An experimental investigation of reflection, transmission and dissipation coefficients associated with regular and irregular waves was carried out. The reflection coefficient was estimated using a least squares method applied to measurements of the water surface elevation from three wave probes. This analysis method assumes that the wave field may be described by linear wave theory and also assumes that there was no frequency scattering in the reflection process. An examination of reflected wave records and a frequency analysis indicated that this assumption about frequency scattering of the reflected wave field is valid.

A series of tests were conducted with a constant water depth d = 0.45 m, and with regular waves with periods ranging from T = 0.6 to 1.6 sec and heights ranging from H = 3.8 cm to 16.7 cm. Some tests were carried out with random waves with Bretschneider spectrum of T_p = 0.6 sec and H_s = 0.05 m. Tests were carried out with a single barrier with two different relative draft values of h/d = 0.5 and 0.1 and with porosities of 0%, 5%, 10%, 20%, 30%, 40% and 50%; and with a pair of barriers with with two different relative draft of h/d = 0.5 and 0.1, with porosities of 0%, 5% and 10% and with three spacing b = 0.2 m, 0.5 m and 1.0 m.

Results from the regular wave tests with a single barrier indicate that the reflection and transmission coefficients, K_r and K_t, are functions of kh, h/d and ε. The results have been compared with the numerical results of Yang (1996) and Kakuno (1983). Yang's model gives good agreement with the experiment results for most of the conditions examined, whereas Kakuno's results gives good agreement only for cases with higher porosity.

Irregular wave tests were undertaken with the objective of determining whether results obtained from regular wave tests would adequately describe the irregular wave transmission. Incident waves corresponding approximately to a Bretschneider spectrum

with a peak frequency f_0 = 1.6 Hz and a significant wave height H_s = 0.05 m. The incident and transmitted wave spectral densities were obtained by analyzing corresponding wave probe signals with a Fourier analysis program. The resulting transmission coefficient function, $K_t(f)$ was estimated from Eq. 2.14 .

In some cases, the spectral density of the incident and transmitted wave train were compared and were seen to be reasonably close in shape. However the peaks of the transmitted spectra were at a lower frequency than those of the incident spectra. The irregular transmission coefficient function $K_t(f)$ was compared with the transmission coefficients measured for the regular wave tests. This comparison shows that there was a good agreement with irregular and regular transmission coefficient except in the case of an impermeable barrier.

Experiments were also carried out with three pairs of vertical barriers separated by distances of 0.2, 0.5 and 1.0 m between the barriers. All other test conditions are the same as in the single barrier experiment. Results from the tests show that the reflection, transmission and energy dissipation coefficients depend on kh, the relative draft h/d, the relative distance between barriers b/h and the porosity ε. The double barrier reduces significantly the transmission when compared to the case of a single barrier. The reflection coefficient does not vary significantly with barrier distance for most of the test conditions. Some experimental results are compared with the numerical results of Yang (1996). This comparison show that Yang's numerical model reasonably predicts the experimental results. Experimental results also exhibits the phenomenon of resonance.

The present study has related to various aspects of wave-structure interaction in the context of single and double, permeable and impermeable, thin vertical wave barriers. It has examined the influence of relative depth, relative draft, relative distance between barriers and porosity on the reflection and transmission coefficients for both regular and random waves. Further experimental studies are needed to investigate the effect of these variables on runup, the wave force and overturning moment acting on the barrier, and to calibrate Yang's (1996) numerical model with respect to these variables as well.

Chapter 5 Conclusions and Recommendations

The influence of oblique waves needs to be assessed and the influence of panel thickness and horizontal slots on the friction and added mass coefficients used in the numerical model also needs to assessed. Finally, it would be desirable to conduct a prototype study inwhich transmission and reflection coefficients are measured for various breakwater and wave parameters.

References

Abul-Azm, A.G. (1993). "Wave diffraction through submerged breakwaters." *Journal of Waterway, Port, Coastal and Ocean Engineering*, ASCE, Vol. 119, No. 6, pp. 587-605.

Bennet, G.S. (1993). "A mathematical model of a slotted wave screen breakwater." *Coastal Engineering*, Vol. 18, pp. 231-249.

Gardner, J.D., Fleming, C.A. and Townend, I.H. (1983). "The design of a slotted vertical screen breakwater." *Proceedings of the Twentieth Coastal Engineering Conference*, Taipei, ASCE, Vol. 2, pp. 1881-1893.

Gilman, J.F. and Dennis, N. (1992). "Wave barriers: an environmentally benign alternative." *Proceedings of Coastal Engineering Practice Conference*, Long Beach, California, ASCE, pp. 479-486.

Hagiwara, K. (1984). "Analysis of upright structure for wave dissipation using integral equation." *Proceedings of the Nineteenth Coastal Engineering Conference*, Houston, Texas, ASCE, Vol. 3, pp. 2810-2826.

Isaacson, M. (1991). "Measurement of regular wave reflection." *Journal of Waterway, Port, Coastal and Ocean Engineering*, ASCE, Vol. 117, No. 6, pp. 553-569.

Isaacson, M. (1996). "Simplified estimation of wave effects on vertical barriers." *Journal of Waterway, Port, Coastal and Ocean Engineering*, ASCE, submitted for publication.

Kakuno, K. (1983). "Reflection and transmission of waves through vertical slit-type structures." *Proceedings of the Coastal Structures Conference*, Arlington, Virginia, ASCE, pp. 939-952.

Liu, P.L-F, and Abbaspour, M. (1982). "Wave scattering by a rigid thin barrier." *Journal of Waterway, Port, Coastal and Ocean Engineering*, ASCE, Vol. 108, No. WW4, pp. 479-491.

Losada, I.J. (1994). "Wave spectrum scattering by vertical thin barriers." *Applied Ocean Research*, Vol. 16, pp. 123-128.

Losada, I.J. (1993). "An analytical method to evaluate the efficiency of porous screens as wave dampers." *Applied Ocean Research*, Vol. 15, pp. 207-215.

Marks, M. and Jarlan, G.E. (1968). "Experimental studies on a fixed perforated breakwater." *Proceedings of the Eleventh Conference on Coastal Engineering*, London, England, ASCE, pp. 1121-1140.

Memos, C.D. and Christodoulou, G.C. (1983). "Forces on a perforated breakwater." *Proceedings of the Coastal Structures Conference*, Arlington, Virginia, ASCE, pp. 573-586.

Sarpkaya, T. and Isaacson, M. (1981). Mechanics of wave forces on offshore structures. Van Nostrand Reinhold, New York.

Terret, F.L., Osorio, J.O.C. and Lean, G.H. (1968). "Model studies of a perforated break water." *Proceedings of the Eleventh Conference on Coastal Engineering*, London, England, ASCE, Vol. 2, pp. 1104-1120.

Wiegel, R.L. (1960). "Transmission of waves past a rigid vertical thin barrier." *Journal of Waterways and Harbours Division*, ASCE, Vol. 86, No. WW1, pp. 1-12.

Yang, G. (1996). Numerical model of wave effects on permeable vertical barriers above seabed. M.A.Sc. thesis, Department of Civil Engineering, University of British Columbia, Vancouver, Canada.

Yu, X. (1996). "Diffraction of water waves by porous breakwaters." *Journal of Waterway, Port, Coastal and Ocean Engineering*, ASCE, Vol. 121, No. 6, pp. 275-282.

Table 1. Summary of wave conditions.

Test Wave	Wave Period (sec)	Wave Height (m)	Wave Steepness	Wave Type
A1	0.6	0.038	0.070	regular
A2	0.8	0.067	0.070	regular
A3	1.0	0.100	0.070	regular
A4	1.2	0.135	0.070	regular
A5	1.4	0.167	0.070	regular
B1	1.0	0.033	0.022	regular
B2	1.0	0.066	0.044	regular
B3	1.0	0.134	0.090	regular
B4	1.6	0.066	0.022	regular
B5	1.6	0.133	0.044	regular
R1	T_p=0.6	0.05	-	irregular

Table 2. Test program for single barrier.

h/d	Porosity (%)	Wave Conditions
1.0	5, 10, 20, 30, 40, 50	A1, A2, A3, A4, A5, B1, B2, B3, B4, B5
	5	R1
0.5	0, 5, 10, 20, 30, 40, 50	A1, A2, A3, A4, A5, B1, B2, B3, B4, B5
	0, 5	R1

Table 3. Test program for double barrier.

h/d	b/h	Porosity(%)	Waves
1.0	2.2, 1.1, 0.44	5, 10	A1, A2, A3, A4, A5, B1, B2, B3, B4, B5
0.5	4.4, 2.3, 0.88	0, 5, 10	A1, A2, A3, A4, A5, B1, B2, B3, B4, B5

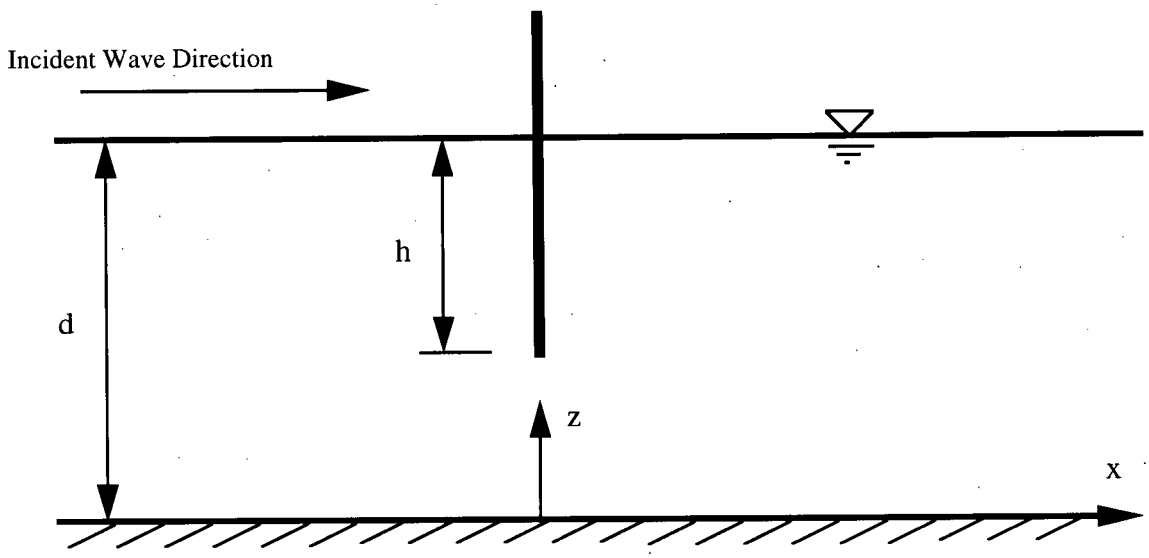

Figure 1. Definition sketch of single barrier.

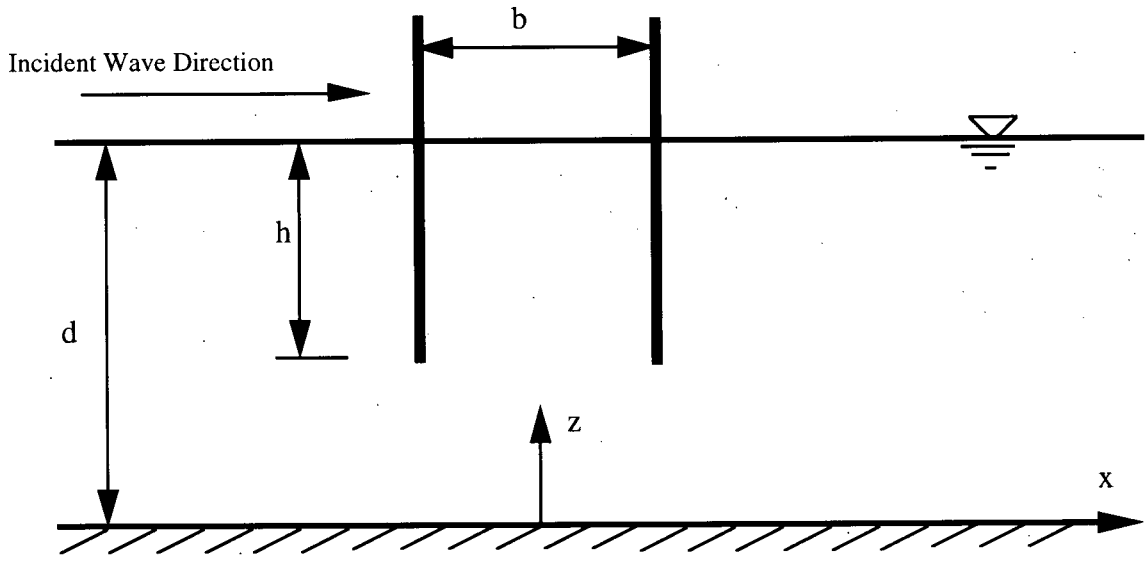

Figure 2. Definition sketch of double barrier.

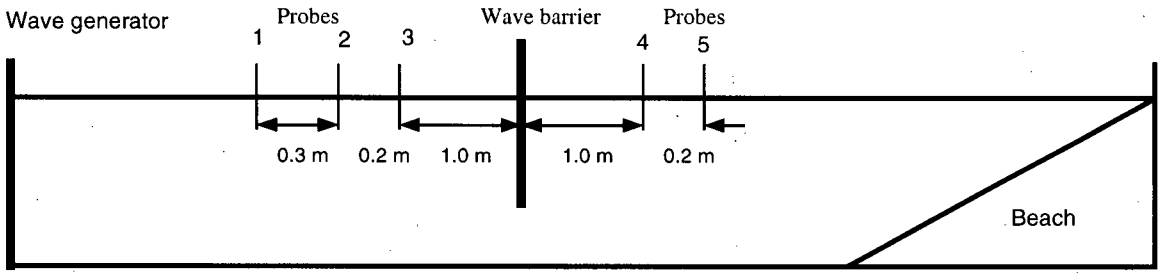

Figure 3. Schematic diagram of experimental setup showing wave probe locations.

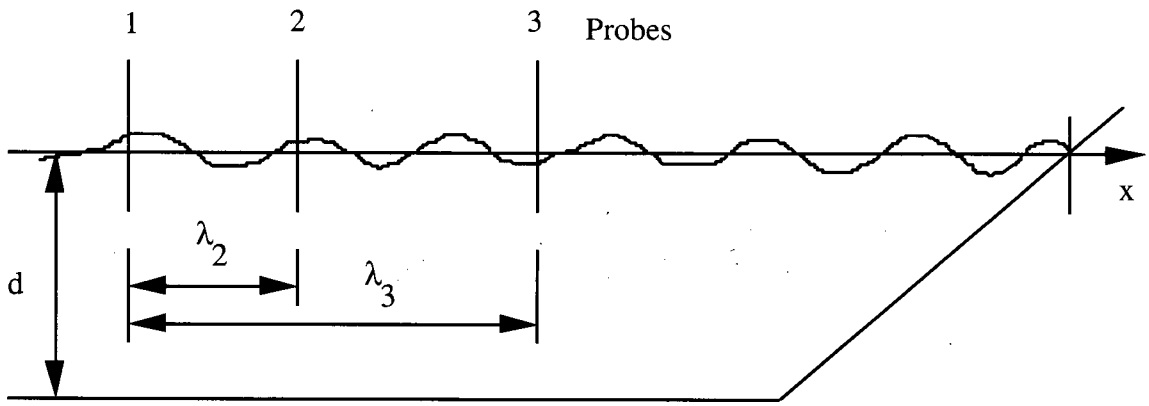

Figure 4. Definition sketch of normal wave reflection.

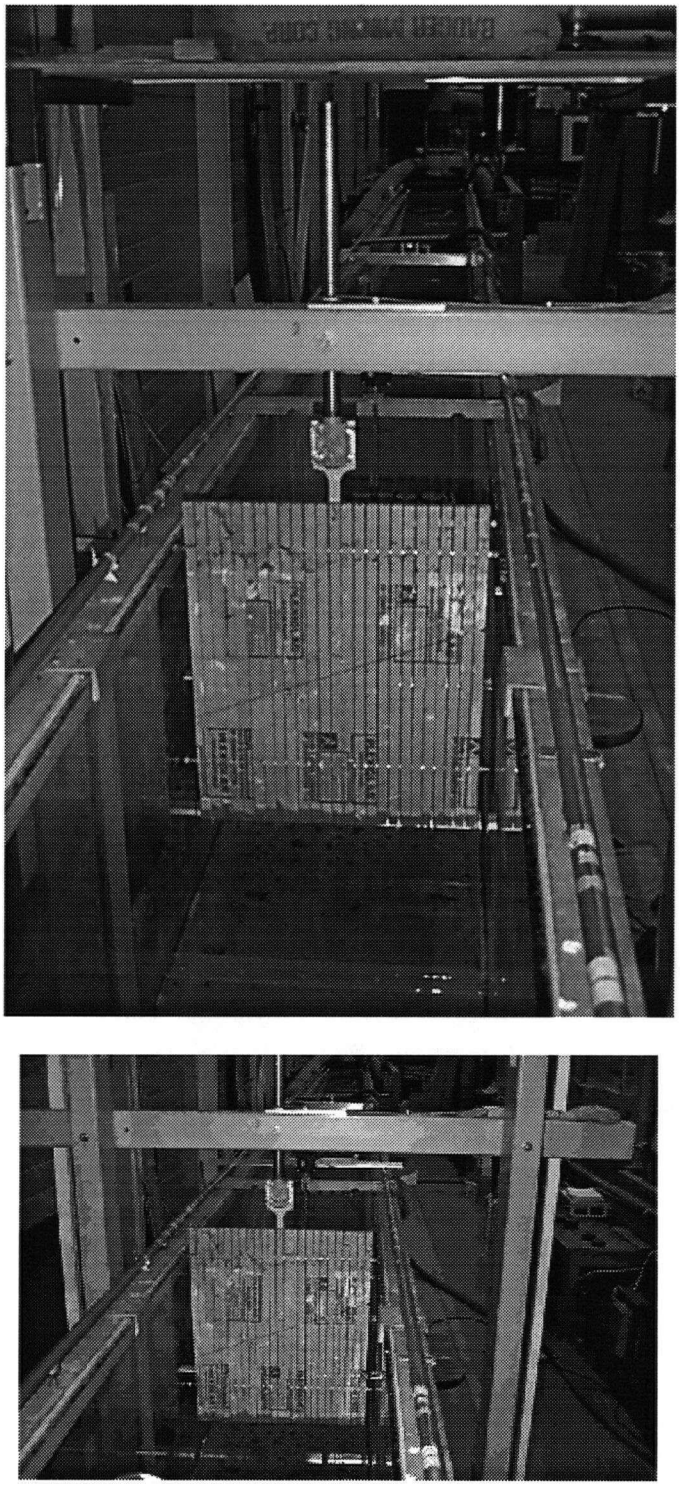

Figure 5. Views of the single barrier in the flume.

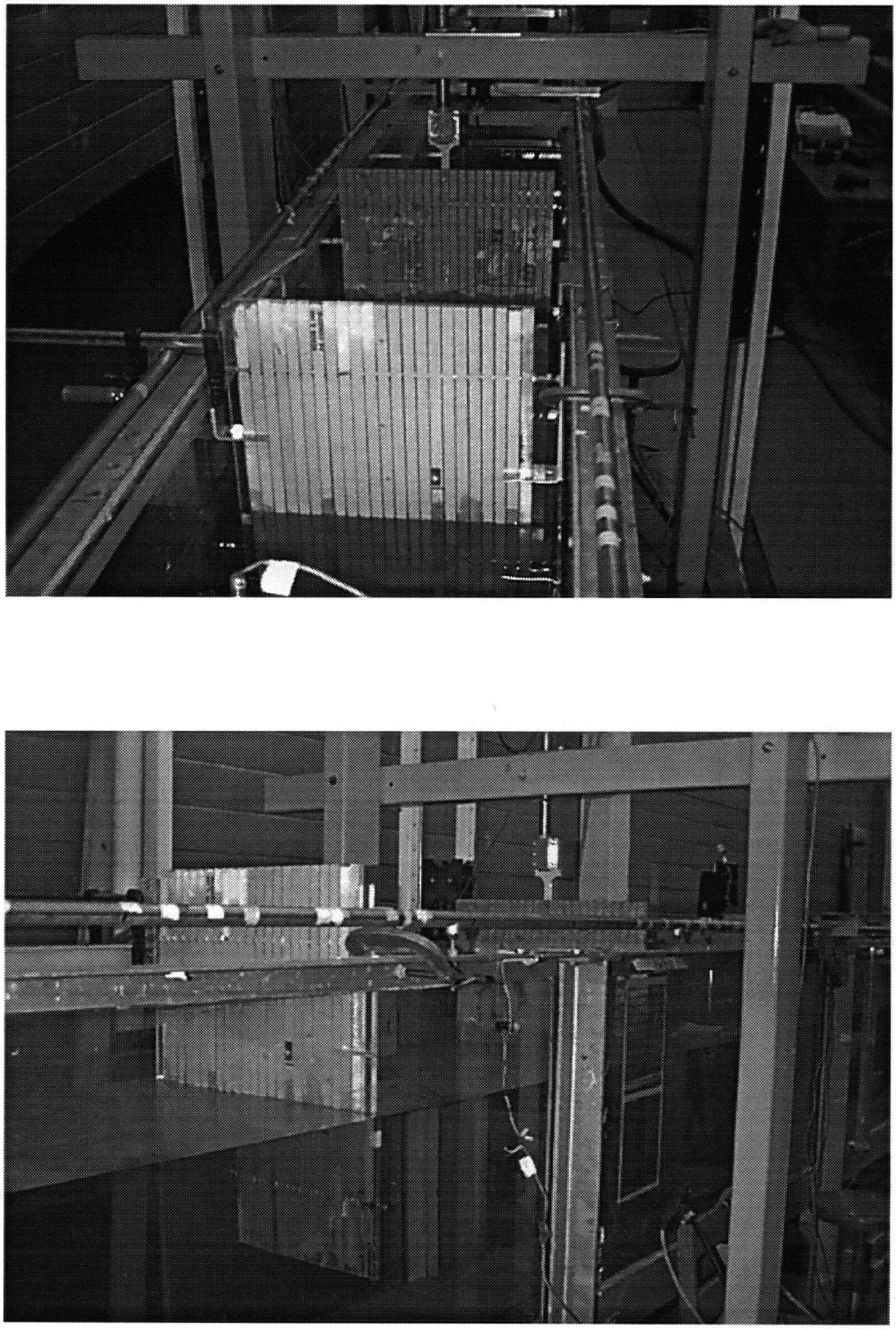

Figure 6. Views of the double barrier in the flume.

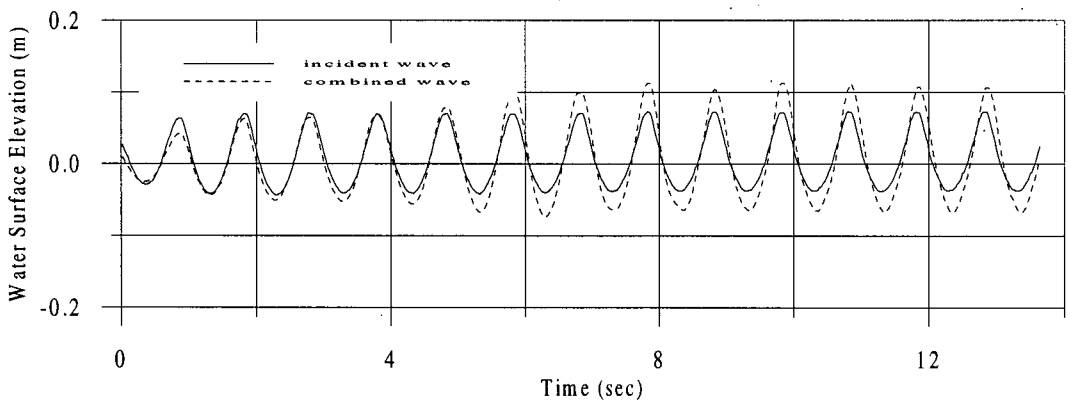

Figure 7. Water surface elevation at probe 1 with and without structure in place

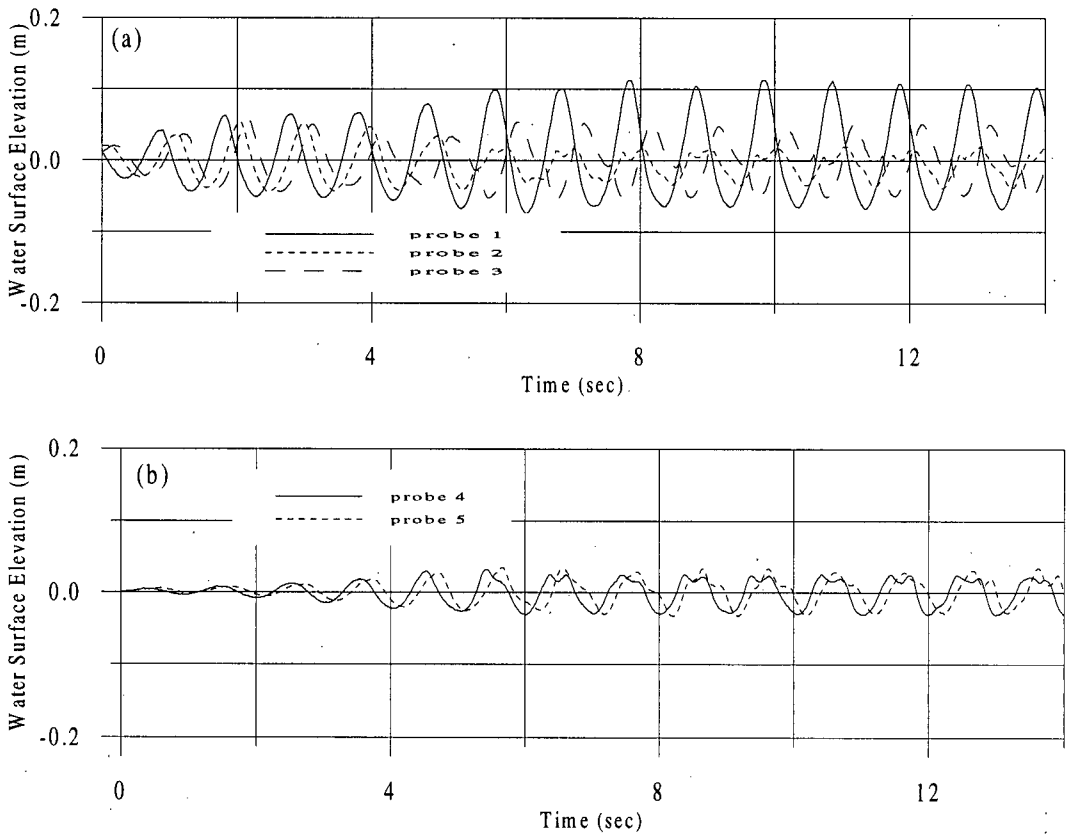

Figure 8. Instantaneous wave profiles with structure in place. (a) upwave side and (b) downwave side

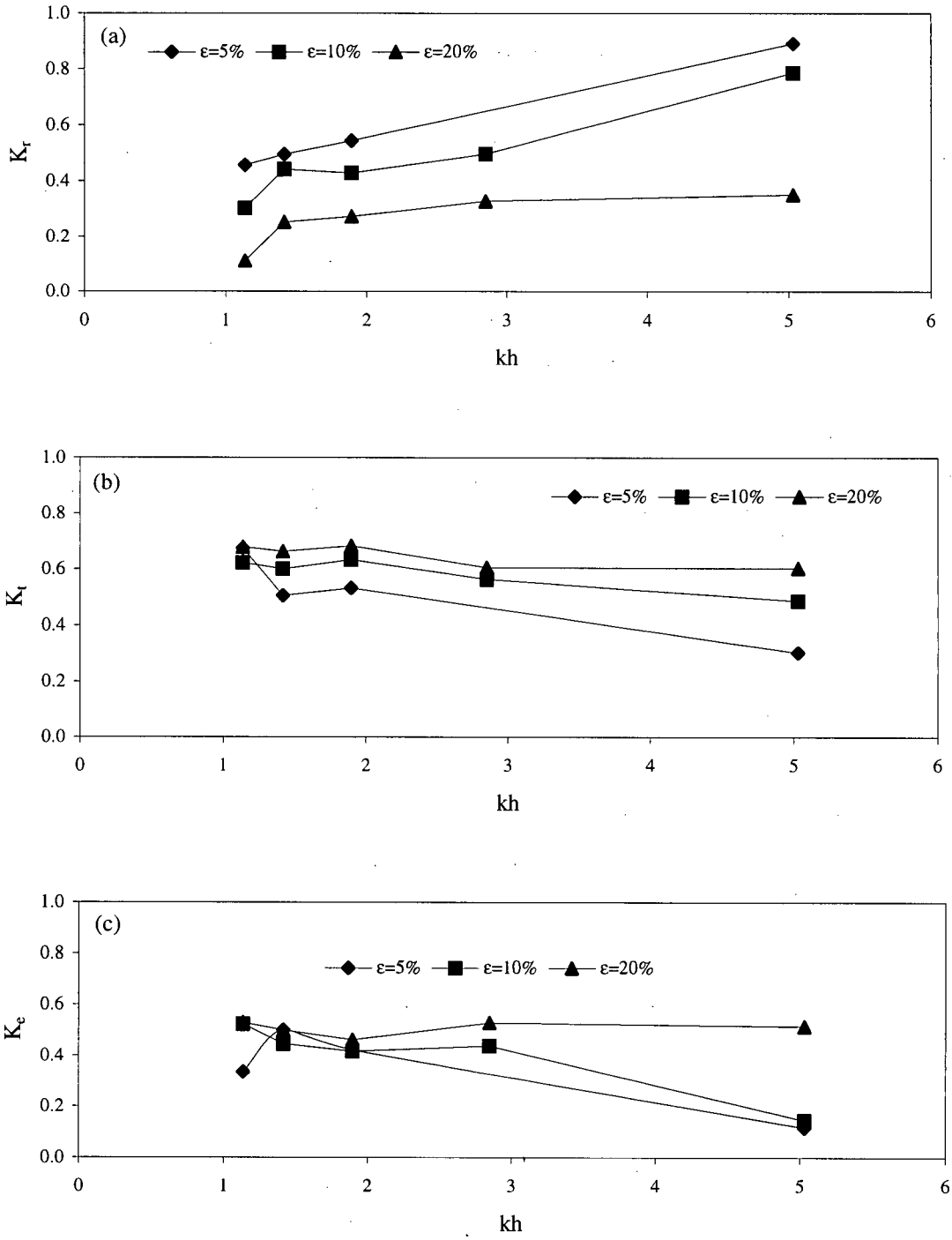

Figure 9. Hydrodynamic coefficients for a single barrier as function of kh for a relative draft h/d = 1.0 and for various porosities. (a) reflection coefficient, (b) transmission coefficient, (c) energy dissipation coefficient.

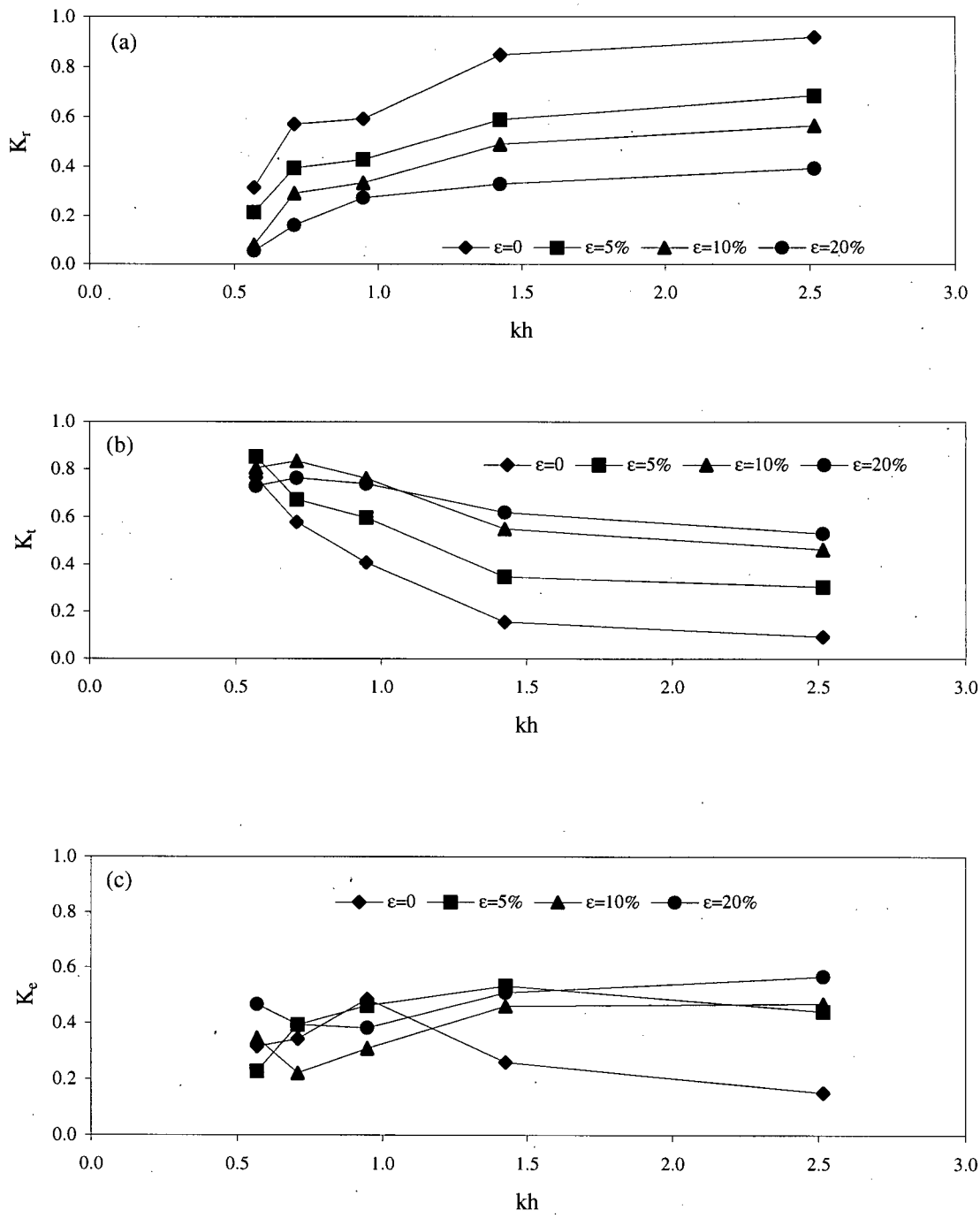

Figure 10. Hydrodynamic coefficients for a single barrier as function of kh for a relative draft h/d = 0.5 and for various porosities. (a) reflection coefficient, (b) transmission coefficient, (c) energy dissipation coefficient.

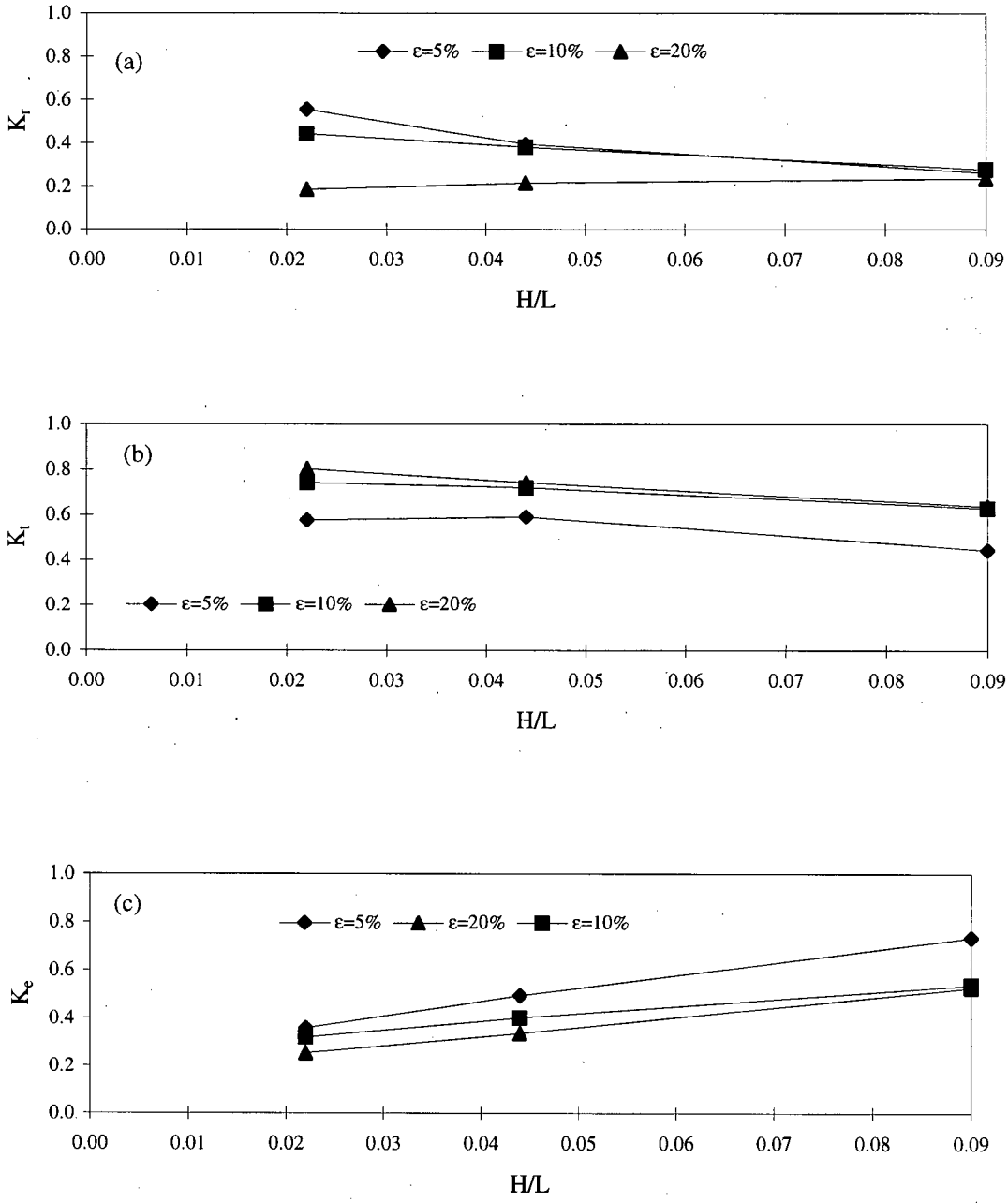

Figure 11. Hydrodynamic coefficients for a single barrier as function of steepness, H/L for a relative draft h/d = 1.0 and kh = 1.9. (a) reflection coefficient, (b) transmission coefficient, (c) energy dissipation coefficient.

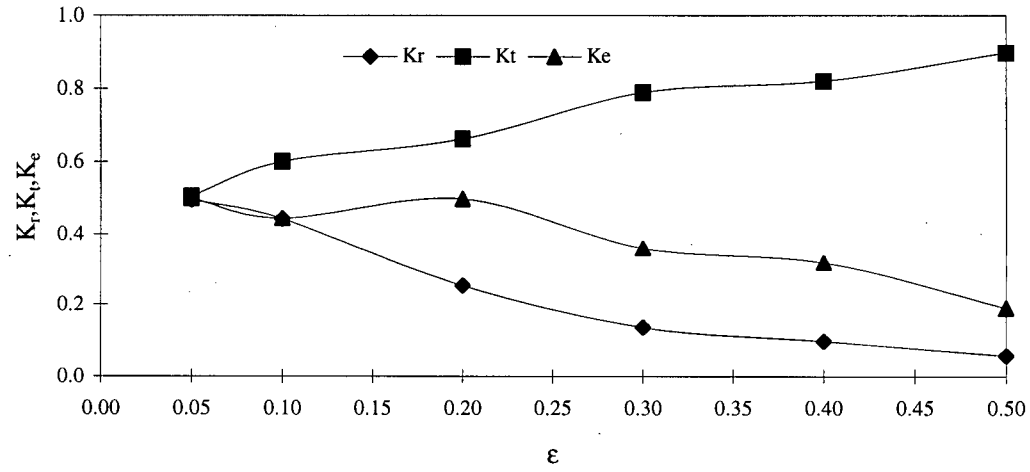

Figure 12. Hydrodynamic coefficients of a single barrier as function of ε for a relative draft h/d = 1.0 and kh = 1.42.

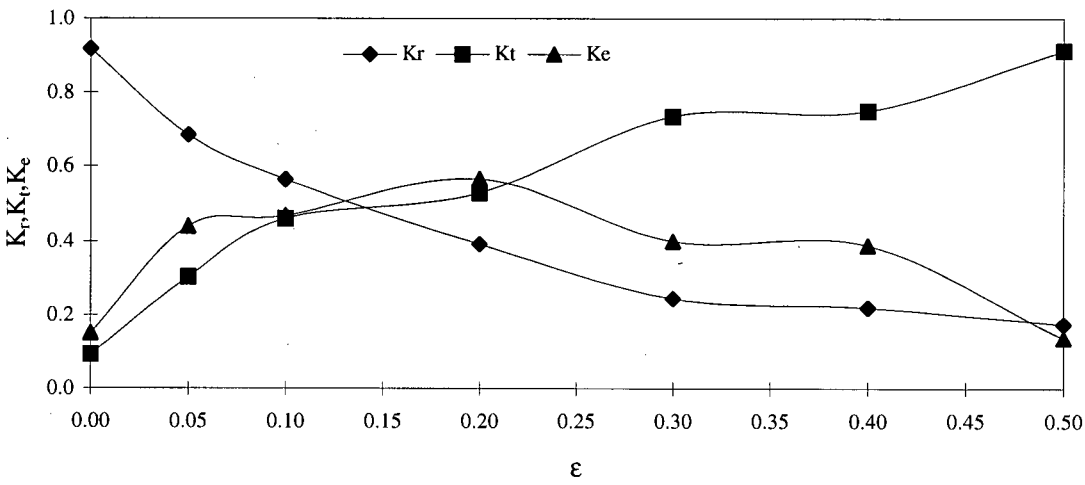

Figure 13. Hydrodynamic coefficients of a single barrier as function of ε for a relative draft h/d = 0.5 and kh = 2.5.

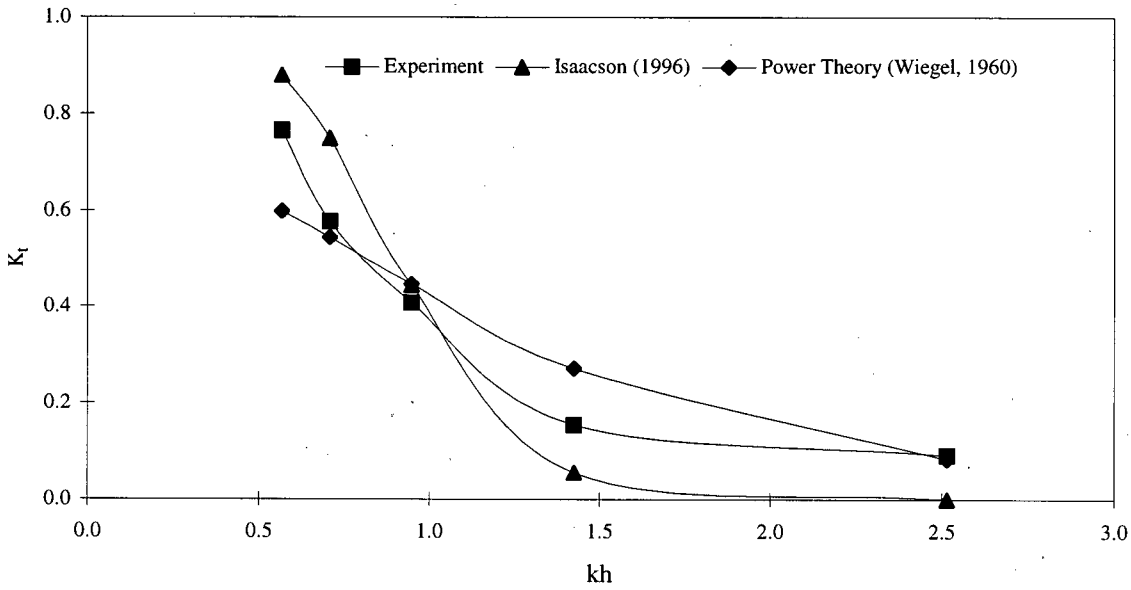

Figure 14. Comparison of transmission coefficient for a single impermeable barrier as a function of kh for a relative draft h/d = 0.5.

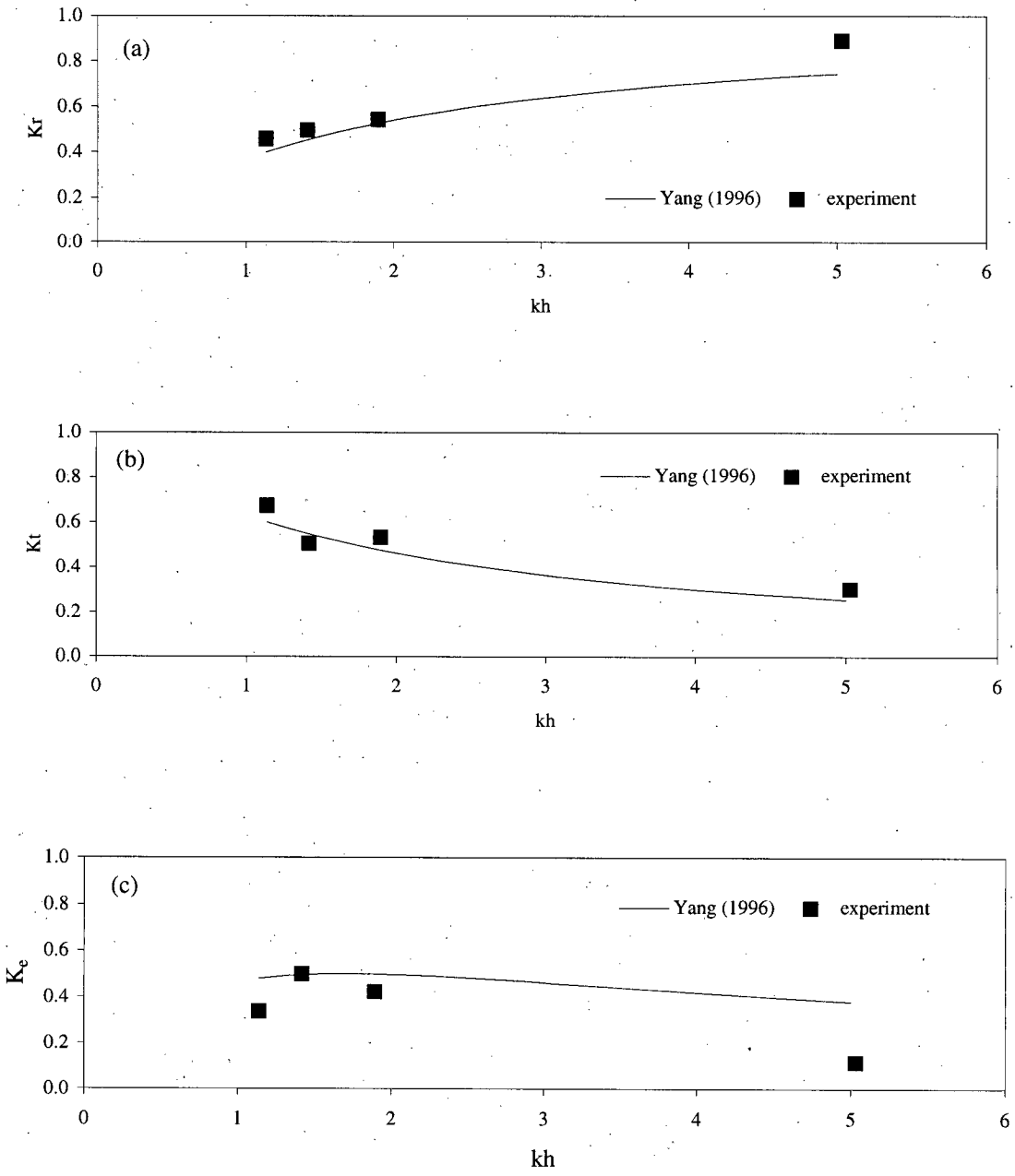

Figure 15. Comparison of hydrodynamic coefficients of a single barrier as function of kh for a relative draft h/d = 1.0 and porosity ε = 5% . (a) reflection coefficient, (b) transmission coefficient, (c) energy dissipation coefficient.

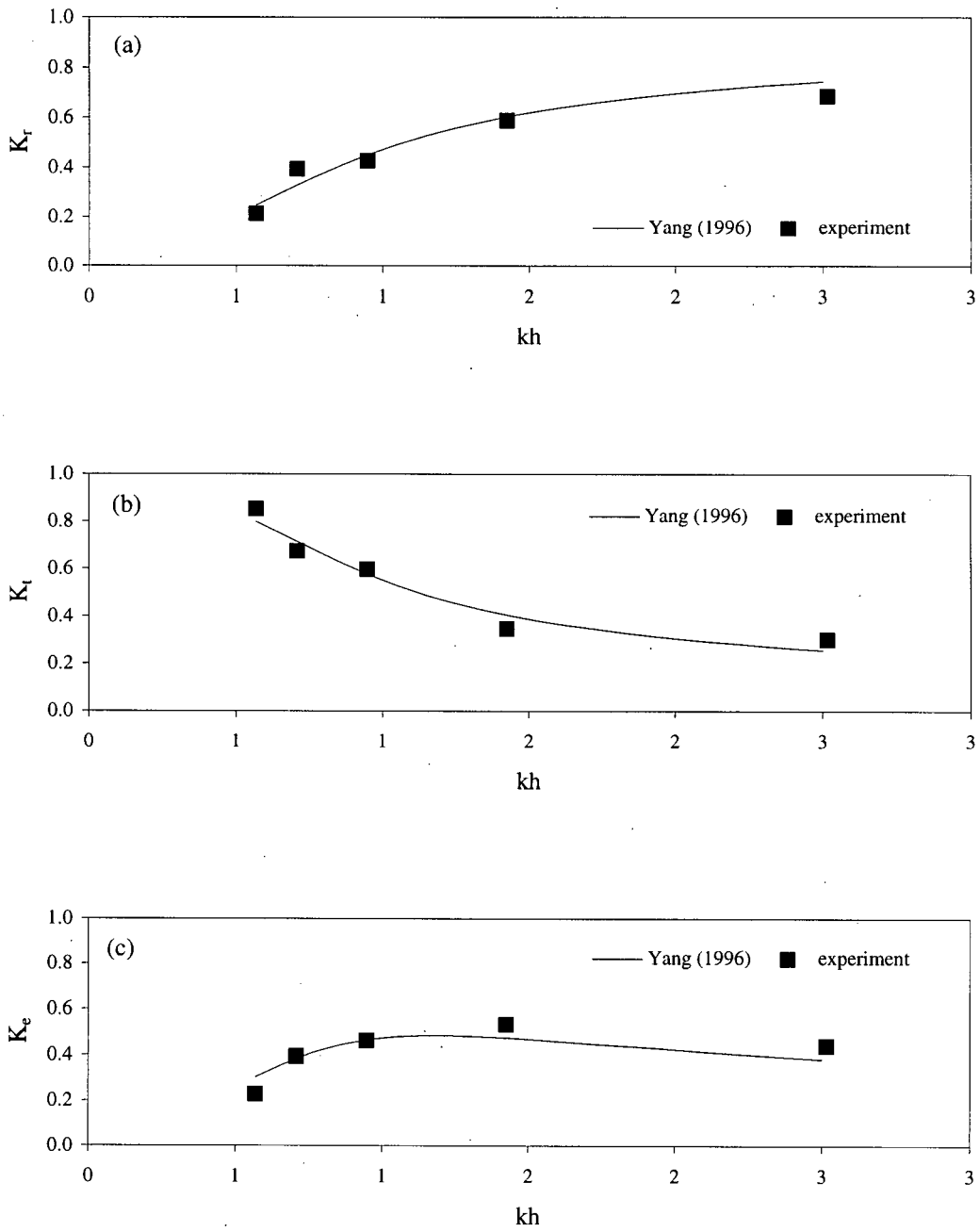

Figure 16. Comparison of hydrodynamic coefficients of a single barrier as function of kh for a relative draft h/d = 0.5 and porosity ε = 5% . (a) reflection coefficient, (b) transmission coefficient, (c) energy dissipation coefficient.

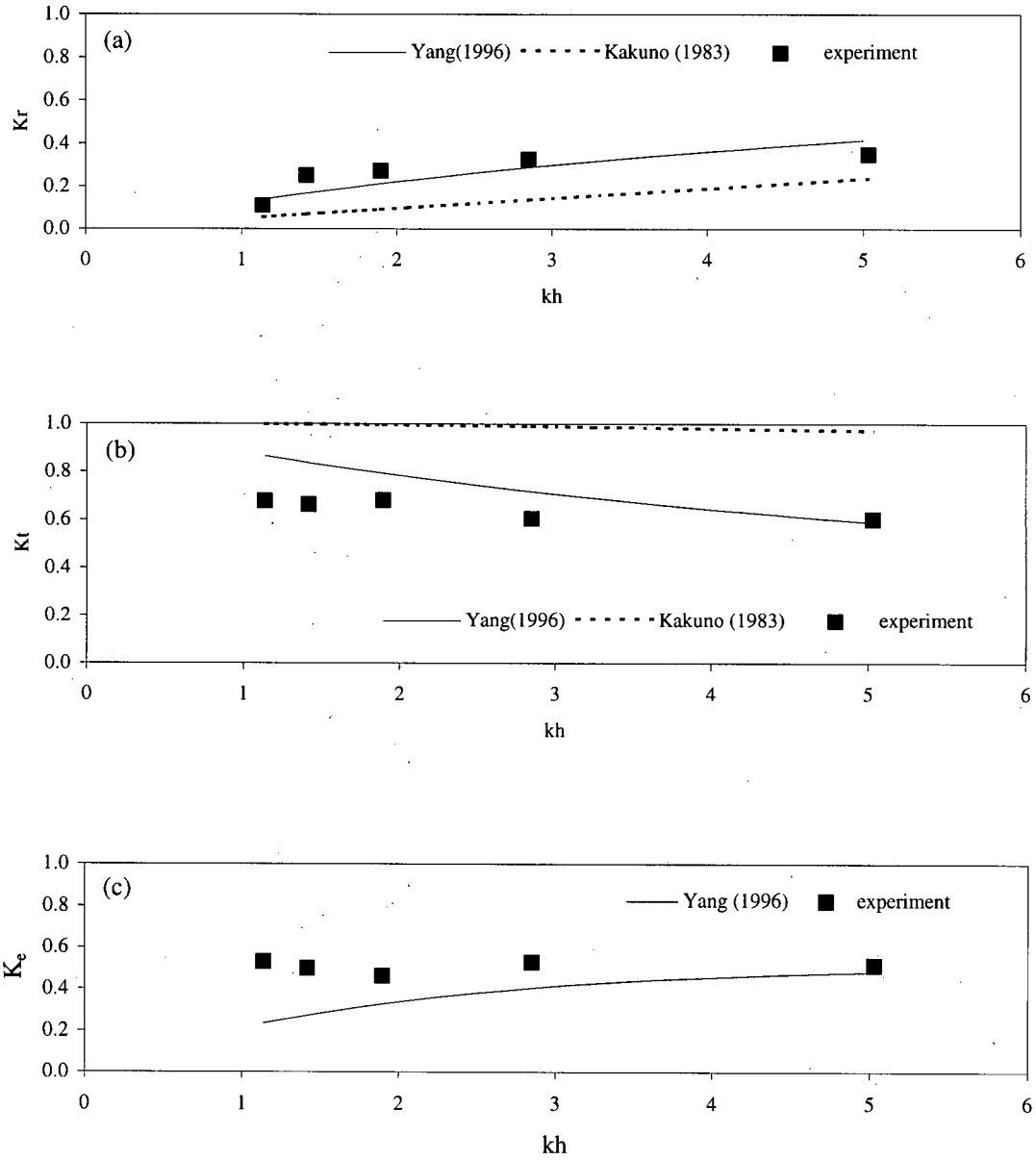

Figure 17. Comparison of hydrodynamic coefficients of a single barrier as function of kh for a relative draft h/d = 1.0 and porosity ε = 20% . (a) reflection coefficient, (b) transmission coefficient, and (c) energy dissipation coefficient.

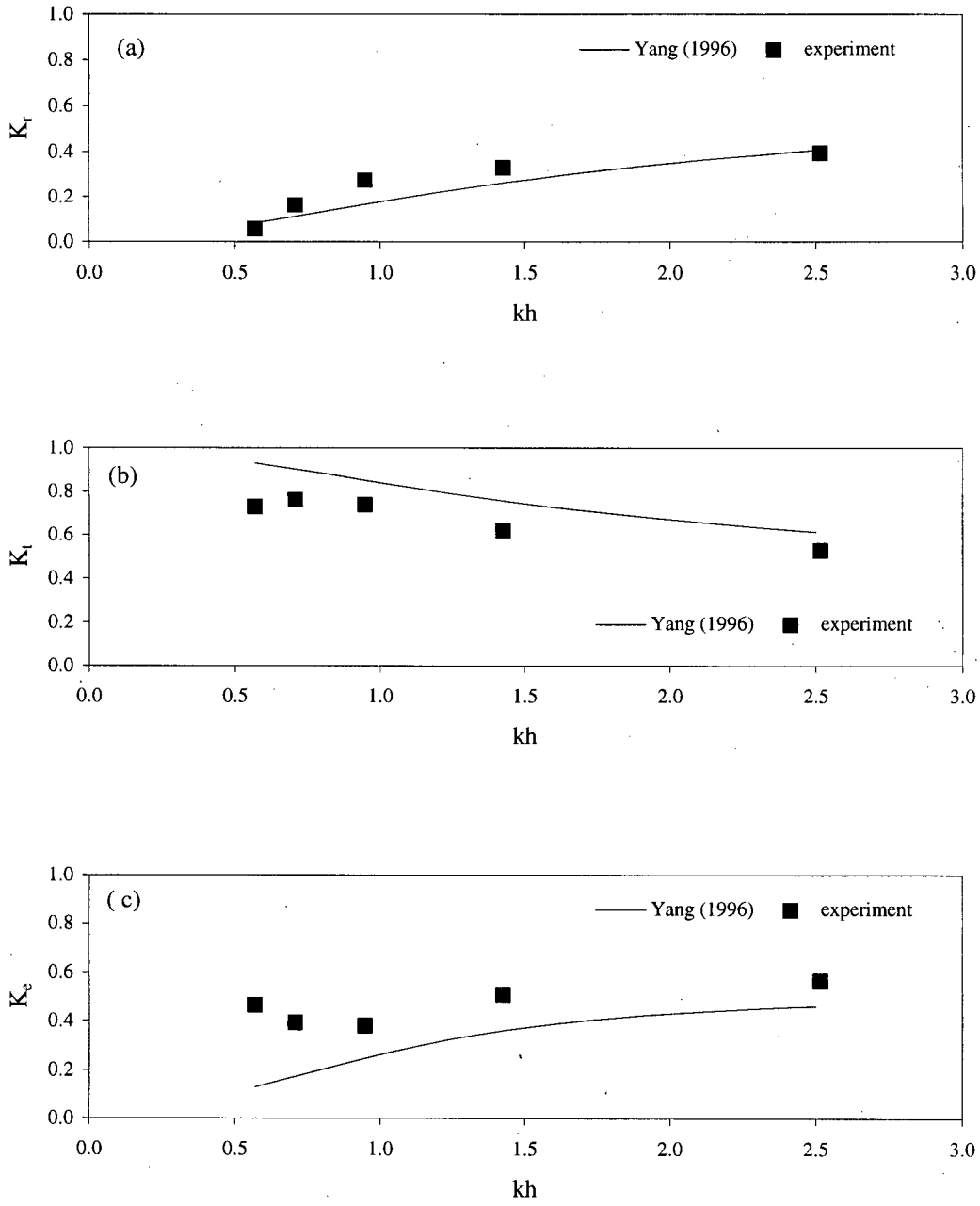

Figure 18. Comparison of hydrodynamic coefficients of a single barrier as function of kh for a relative draft h/d = 0.5 and porosity ε = 20% . (a) reflection coefficient, (b) transmission coefficient, (c) energy dissipation coefficient.

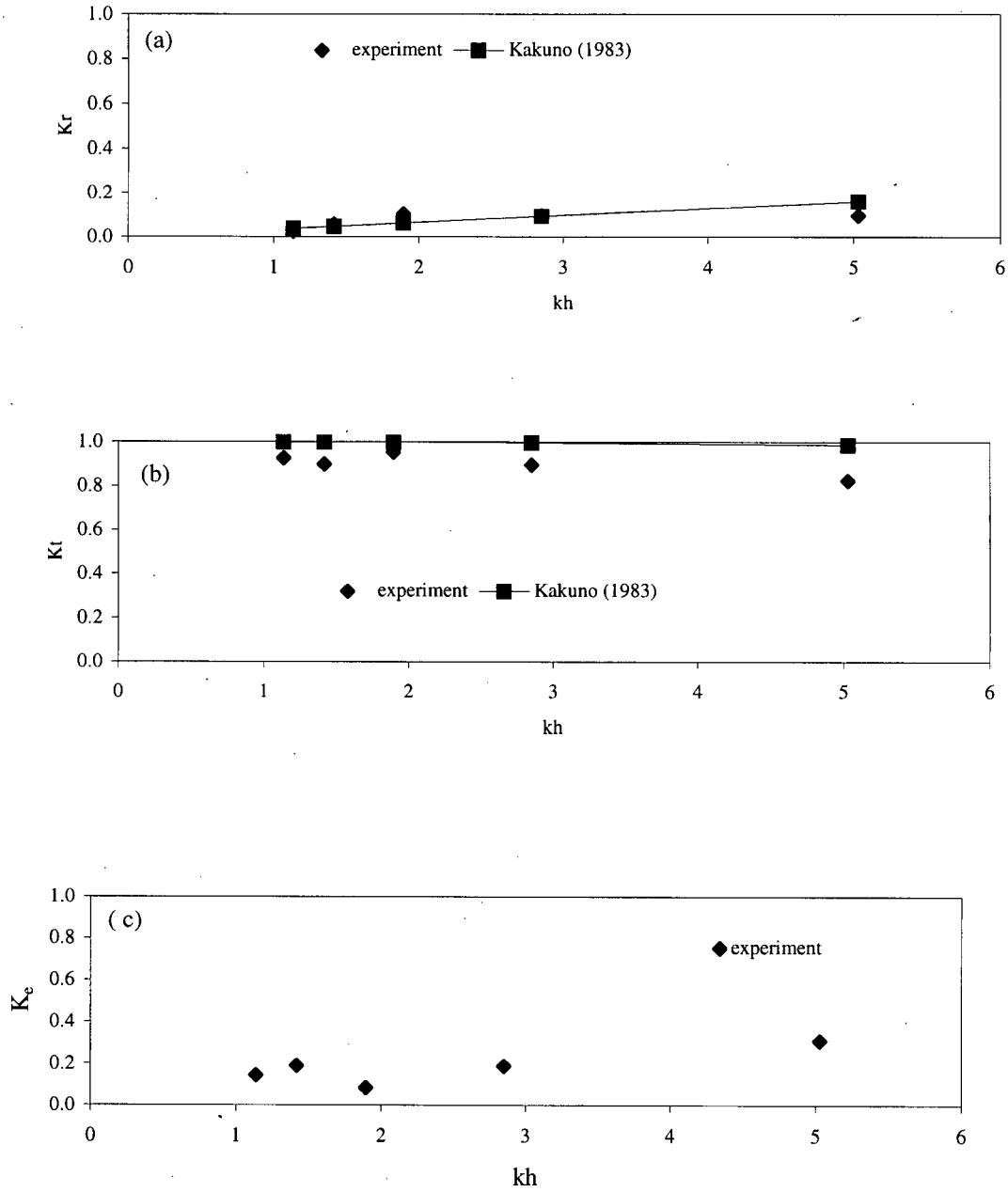

Figure 19. Comparison of hydrodynamic coefficients of a single barrier as function of kh for a relative draft h/d = 1.0 and porosity ε = 50% . (a) reflection coefficient, (b) transmission coefficient, (c) energy dissipation coefficient.

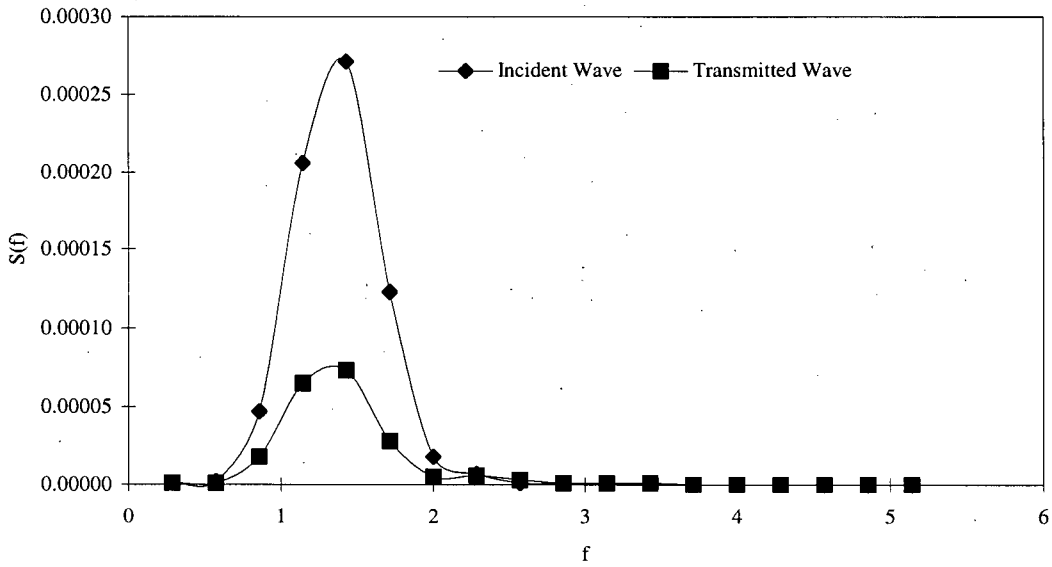

Figure 20. Incident and transmitted spectral density for a relative draft h/d = 1.0 and porosity ε = 10%(Bretschneider spectrum, T_p = 0.6 sec and H_s = 0.05 m).

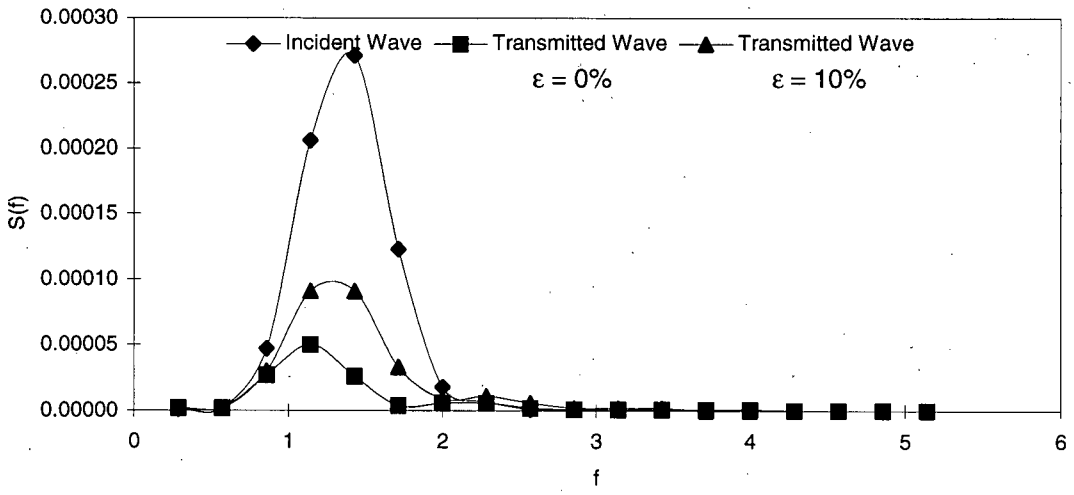

Figure 21. Incident and transmitted spectral density for a relative draft h/d = 0.5 (Bretschneider spectrum, T_p = 0.6 sec and H_s = 0.05 m).

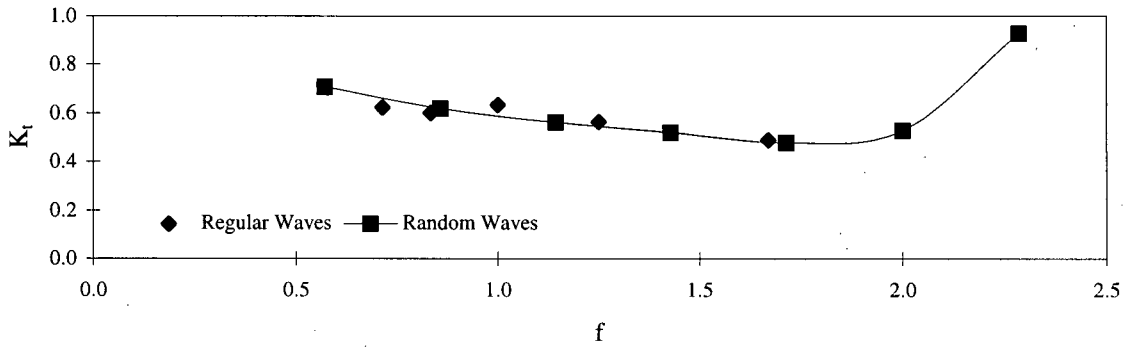

Figure 22. Comparison of regular and irregular wave transmission for a relative draft h/d = 1.0 and porosity ε = 10%.

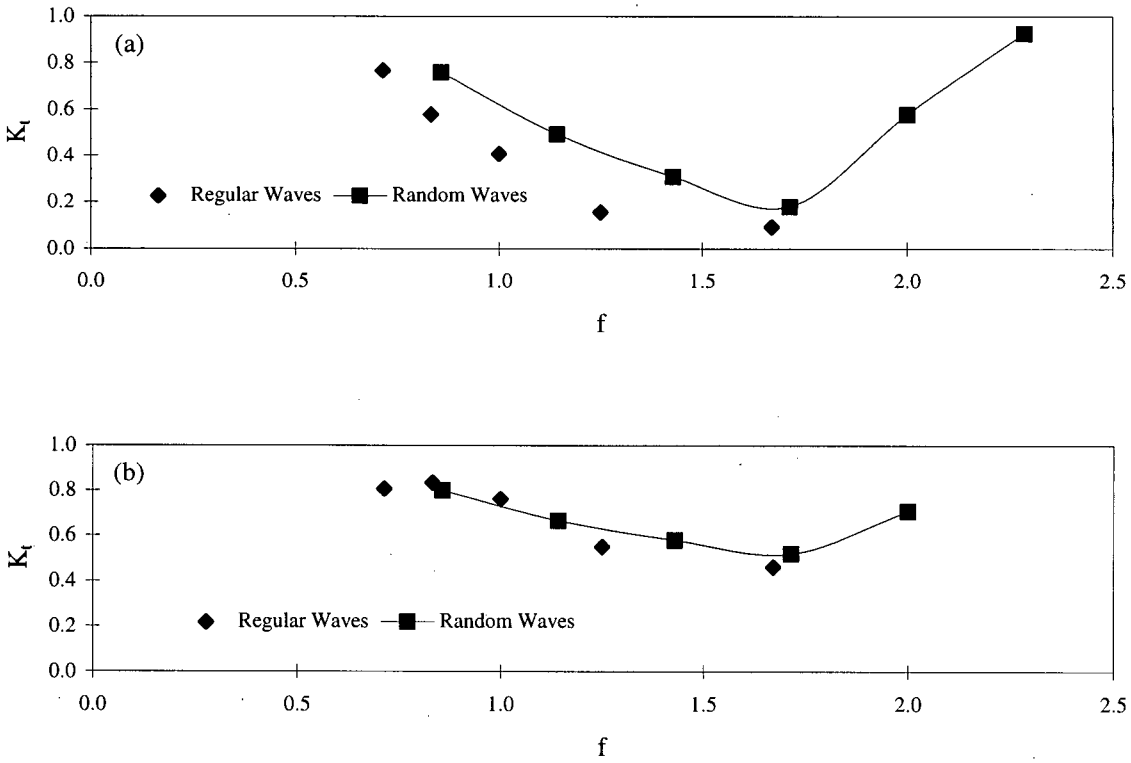

Figure 23. Comparison of regular and irregular wave transmission for relative draft h/d = 0.5 (a) porosity ε = 0%, and (b) porosity ε = 10%.

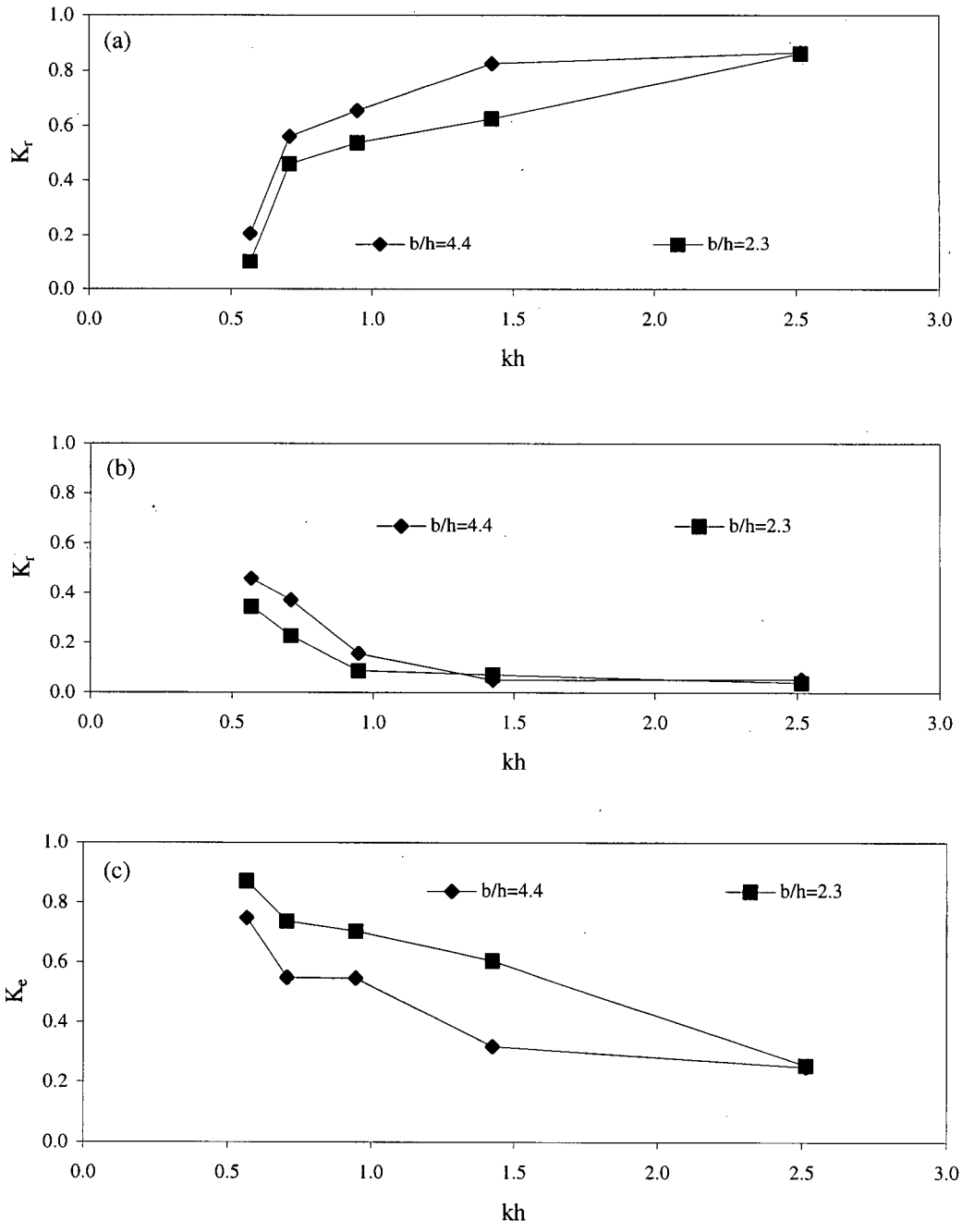

Figure 24. Hydrodynamic coefficients for a double barrier as function of kh for a relative draft h/d = 0.5 and porosity ε = 0% . (a) reflection coefficient, (b) transmission coefficient, (c) energy dissipation coefficient.

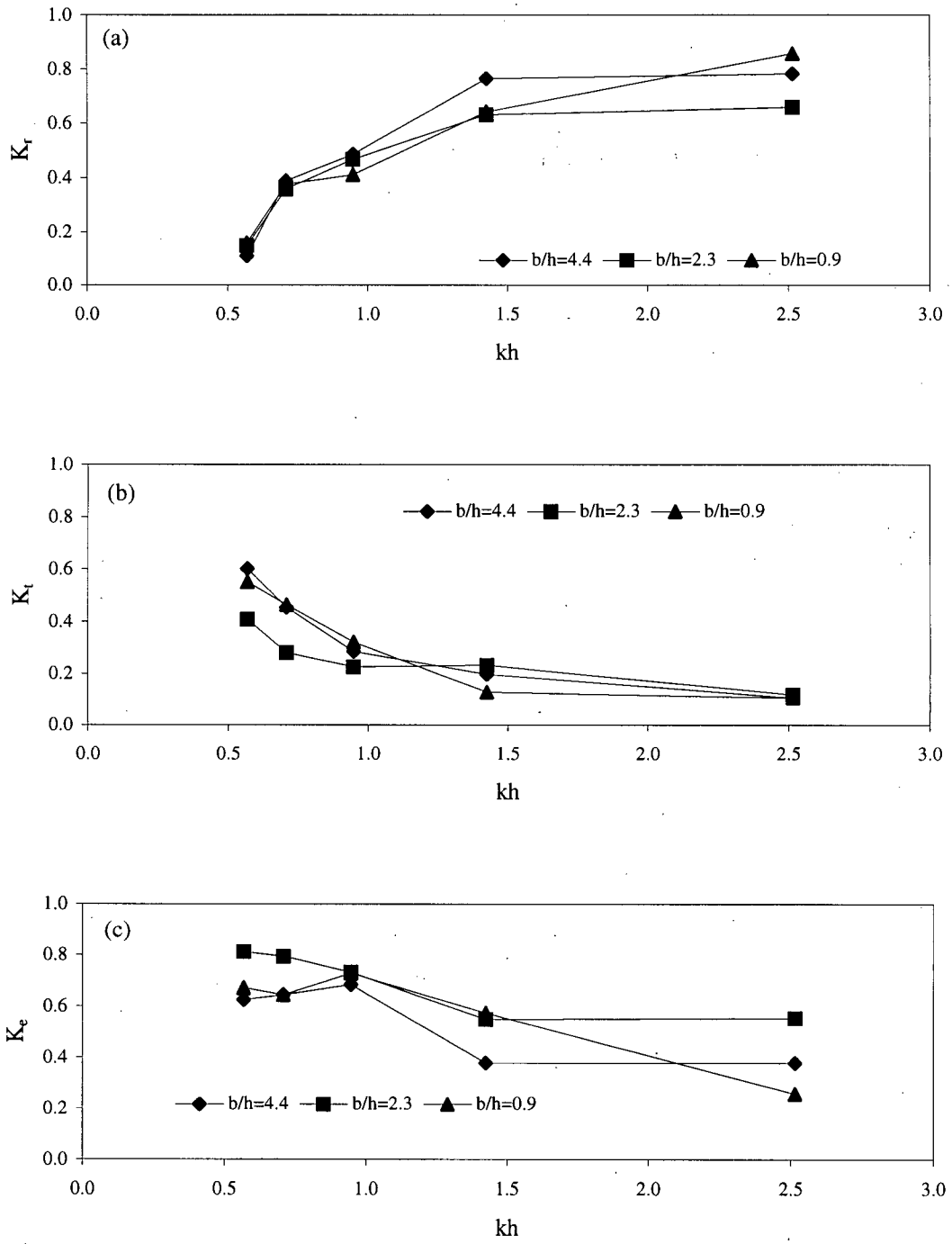

Figure 25. Hydrodynamic coefficients for a double barrier as function of kh for a relative draft h/d = 0.5 and porosity ε = 5% . (a) reflection coefficient, (b) transmission coefficient, (c) energy dissipation coefficient.

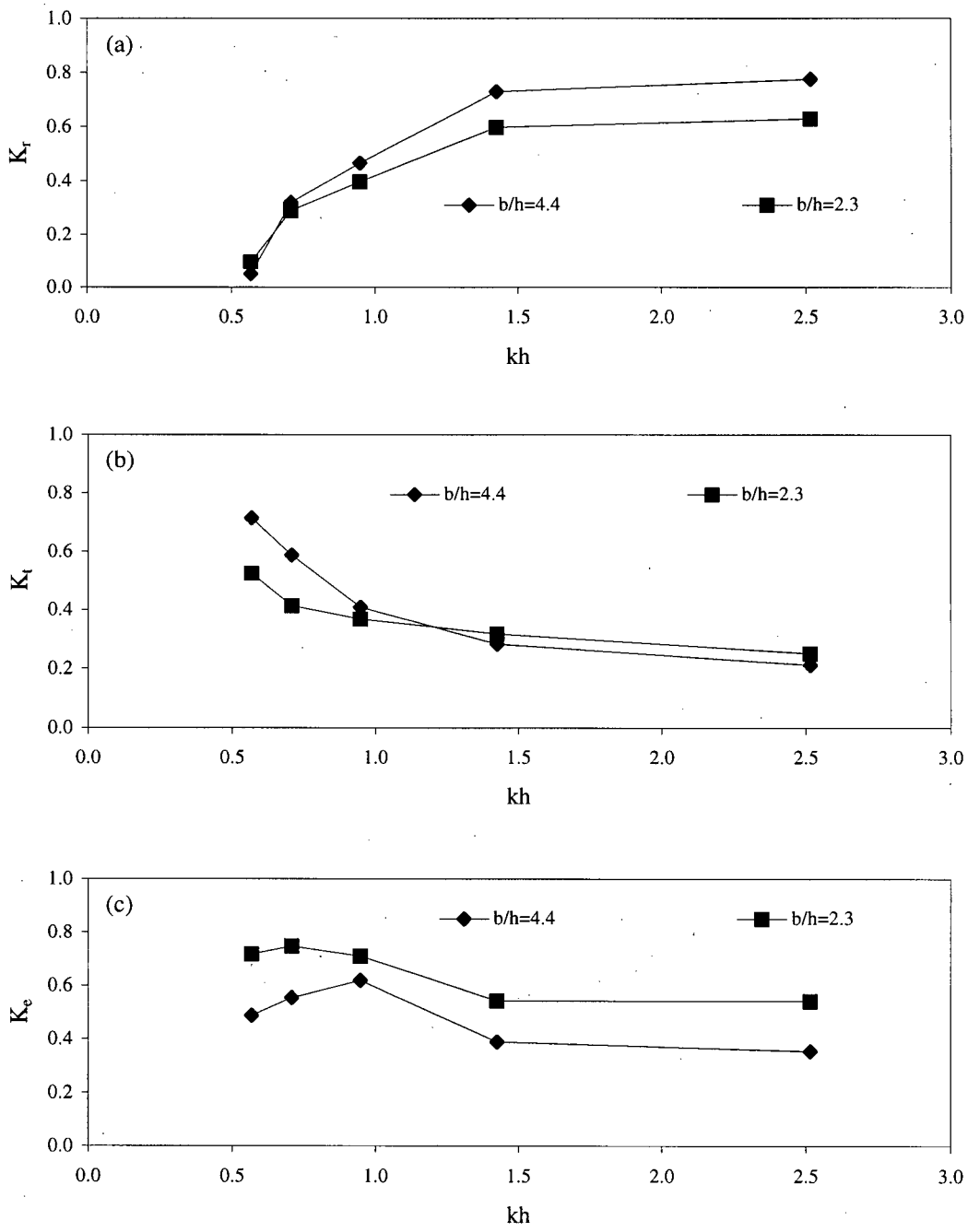

Figure 26. Hydrodynamic coefficients for a double barrier as function of kh for a relative draft h/d = 0.5 and porosity ε = 10% . (a) reflection coefficient, (b) transmission coefficient, (c) energy dissipation coefficient.

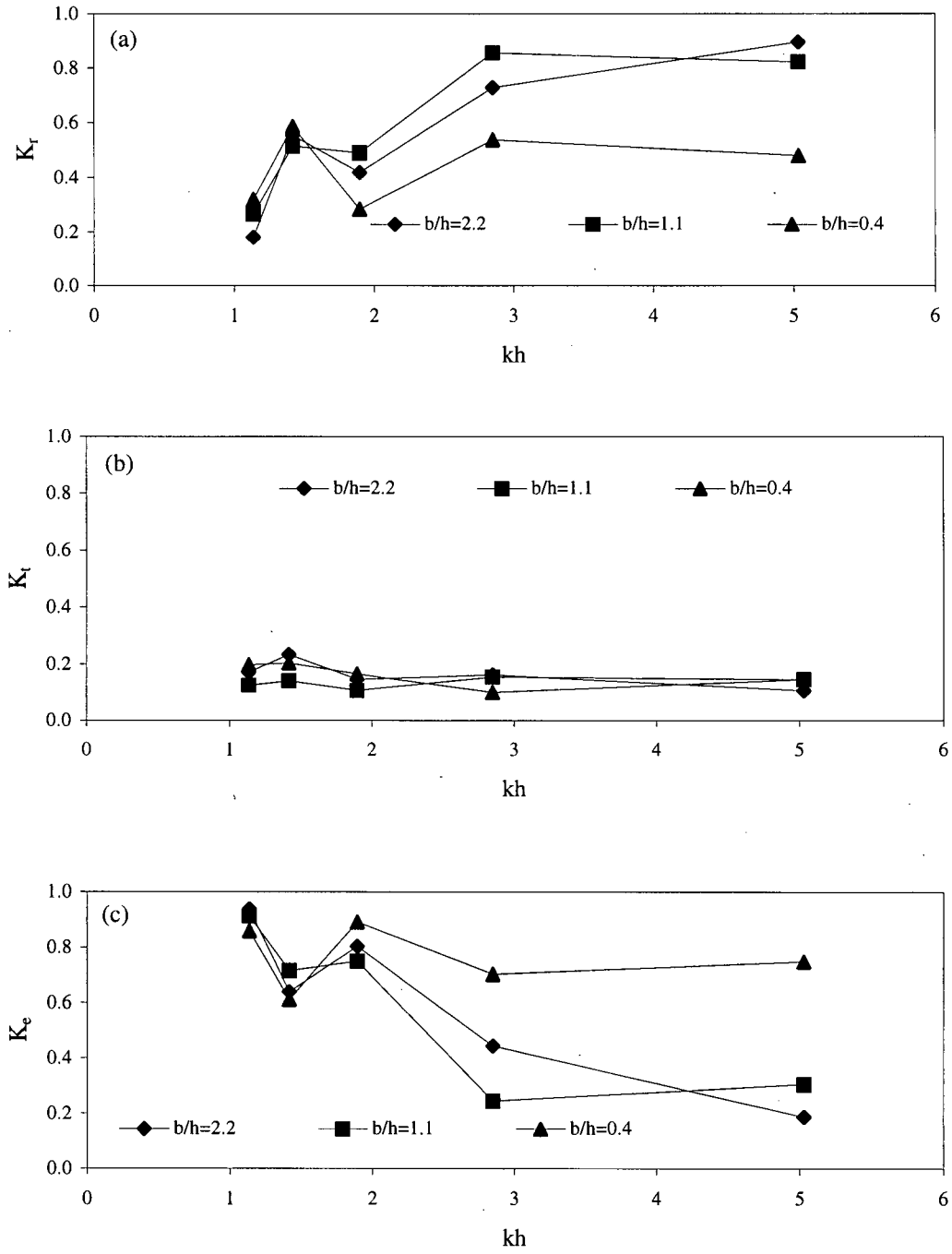

Figure 27. Hydrodynamic coefficients for a double barrier as function of kh for a relative draft h/d = 1.0 and porosity ε = 5% . (a) reflection coefficient, (b) transmission coefficient, (c) energy dissipation coefficient.

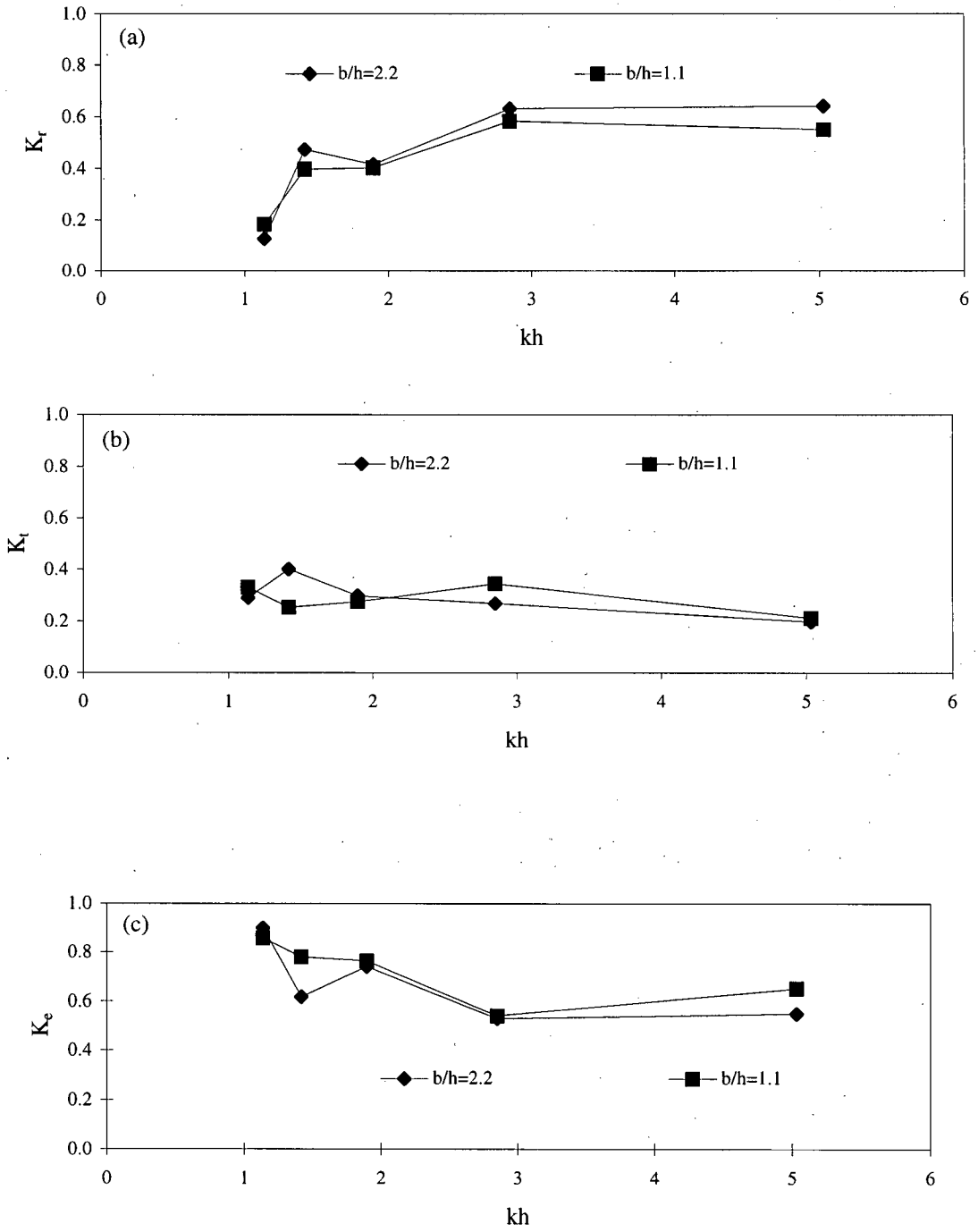

Figure 28. Hydrodynamic coefficients for a double barrier as function of kh for a relative draft h/d = 1.0 and porosity ε = 10% . (a) reflection coefficient, (b) transmission coefficient, (c) energy dissipation coefficient.

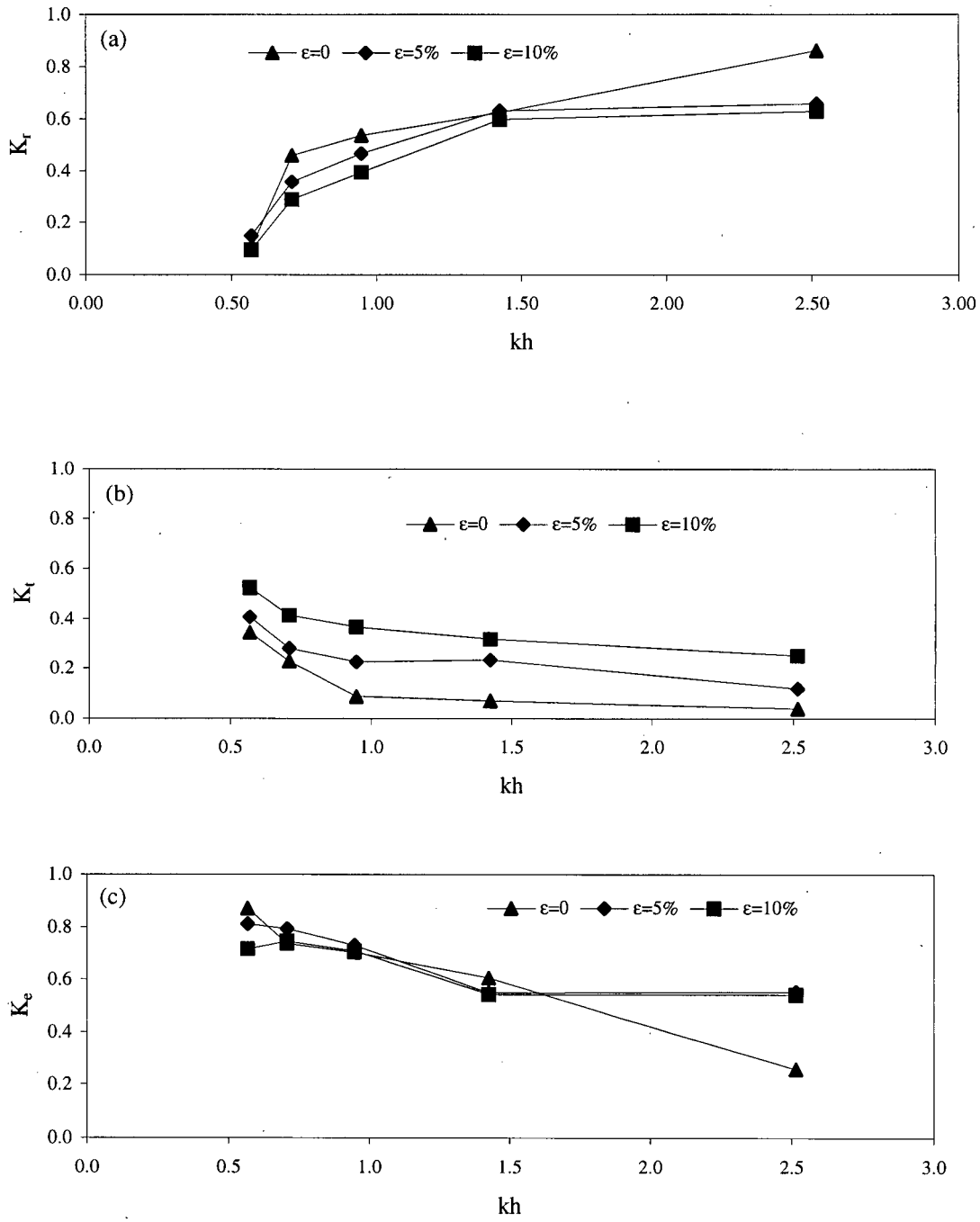

Figure 29. Hydrodynamic coefficients for a double barrier as function of kh for a relative draft h/d = 0.5 and relative distance b/h = 2.2. (a) reflection coefficient, (b) transmission coefficient, (c) energy dissipation coefficient.

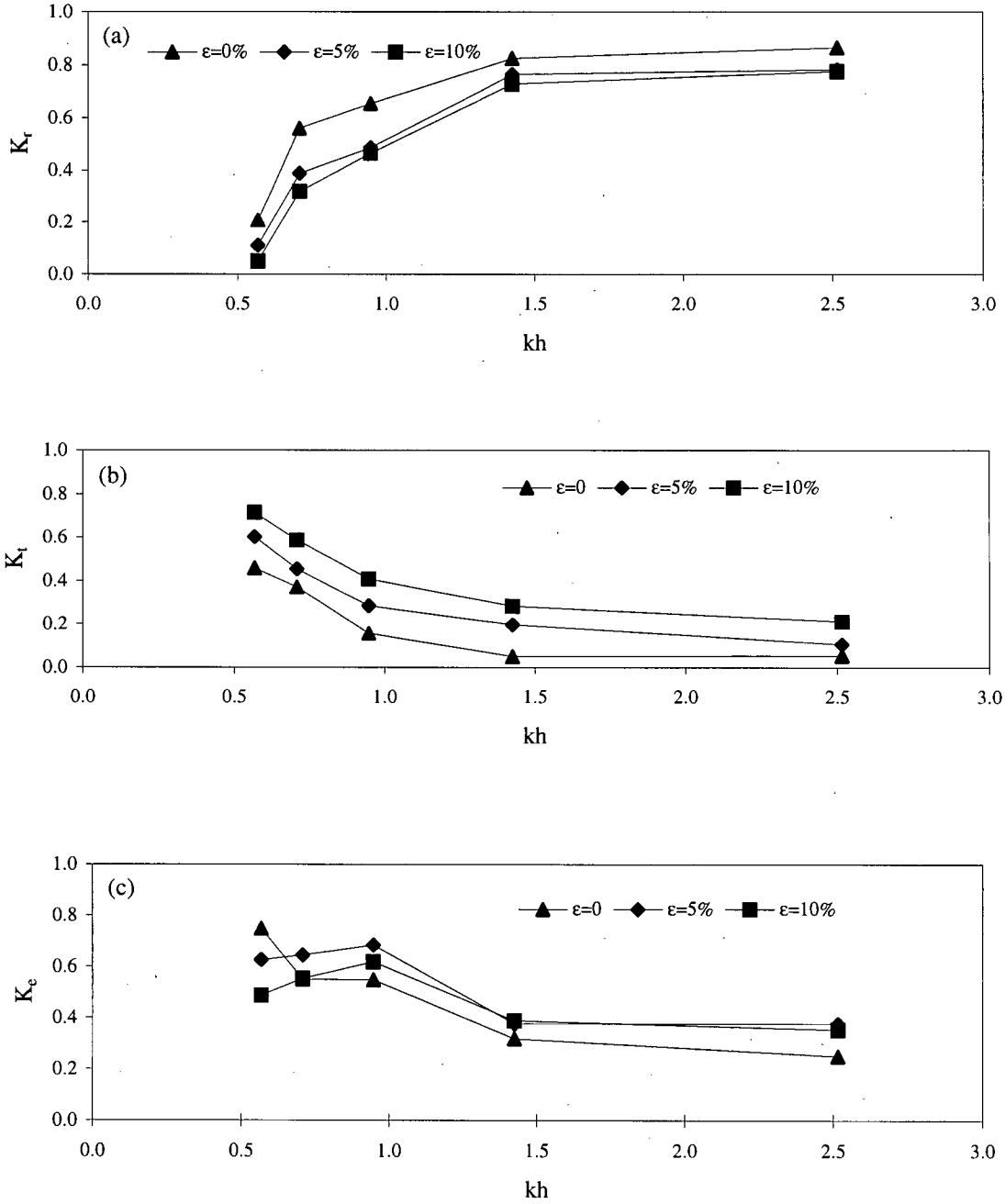

Figure 30. Hydrodynamic coefficients for a double barrier as function of kh for a relative draft h/d = 0.5 and relative distance b/h = 4.4. (a) reflection coefficient, (b) transmission coefficient, and (c) energy dissipation coefficient.

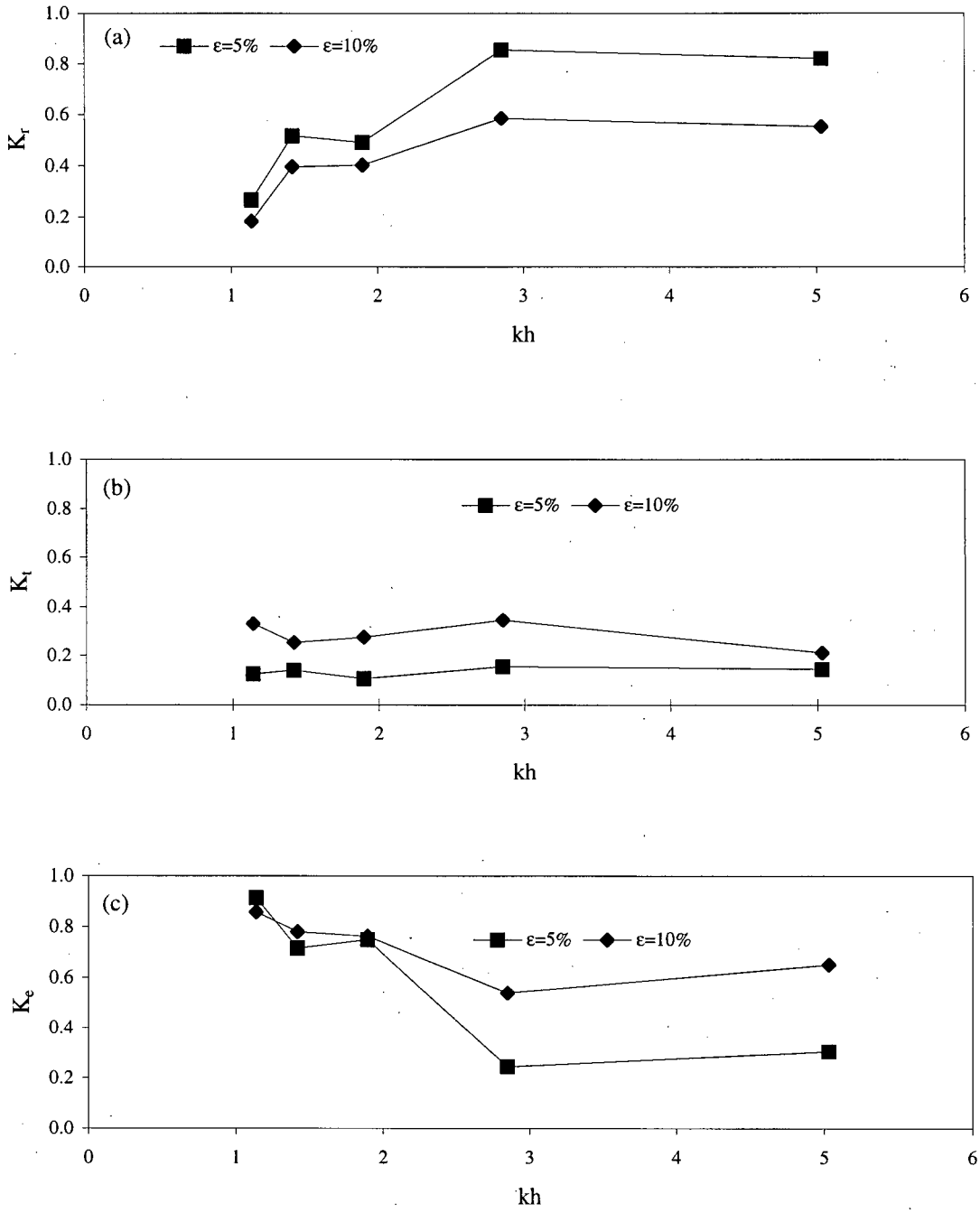

Figure 31. Hydrodynamic coefficients for a double barrier as function of kh for a relative draft h/d = 1.0 and relative distance b/h = 1.1. (a) reflection coefficient, (b) transmission coefficient, and (c) energy dissipation coefficient.

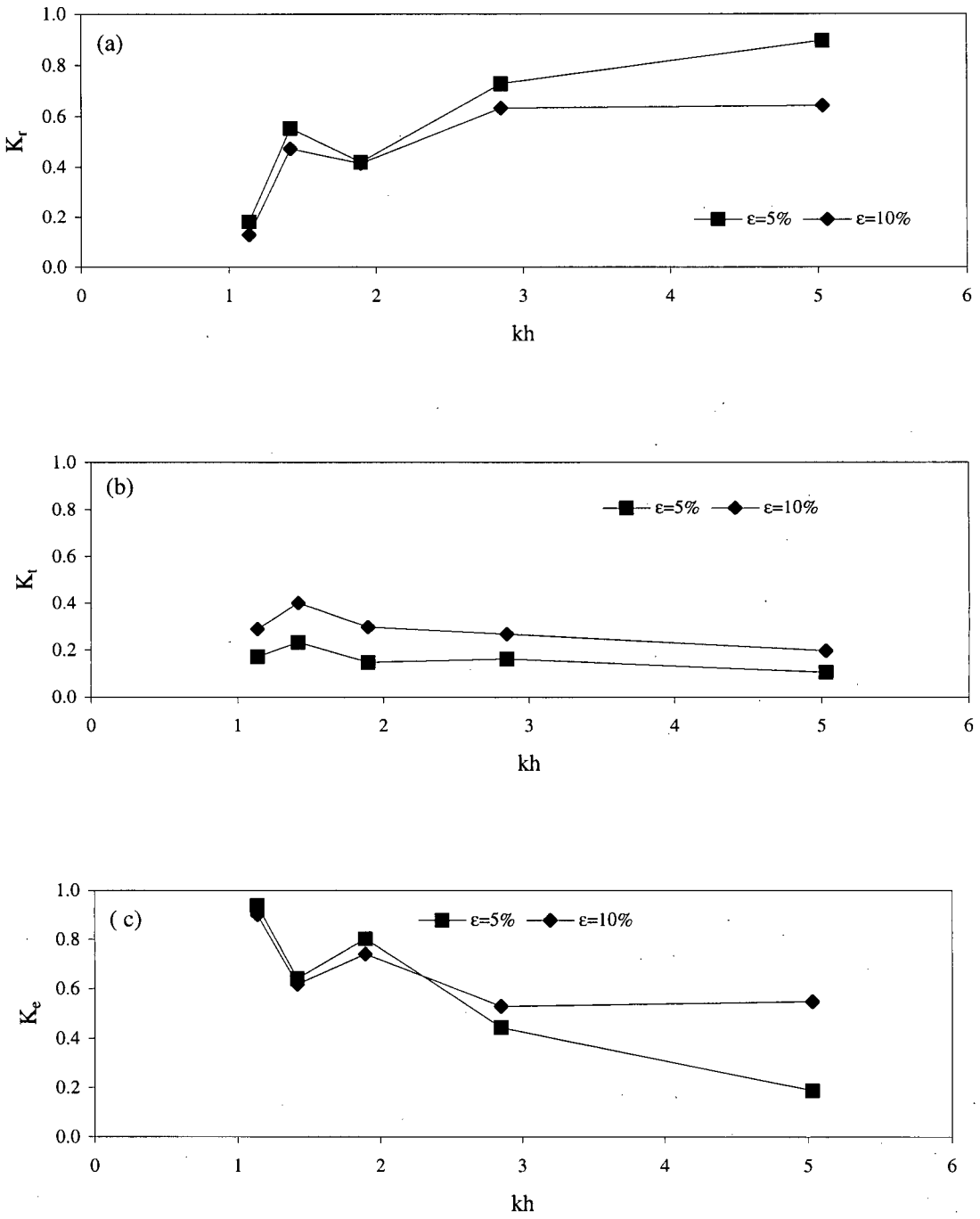

Figure 32. Hydrodynamic coefficients for a double barrier as function of kh for a relative draft h/d = 1.0 and relative distance b/h = 2.2. (a) reflection coefficient, (b) transmission coefficient, (c) energy dissipation coefficient.

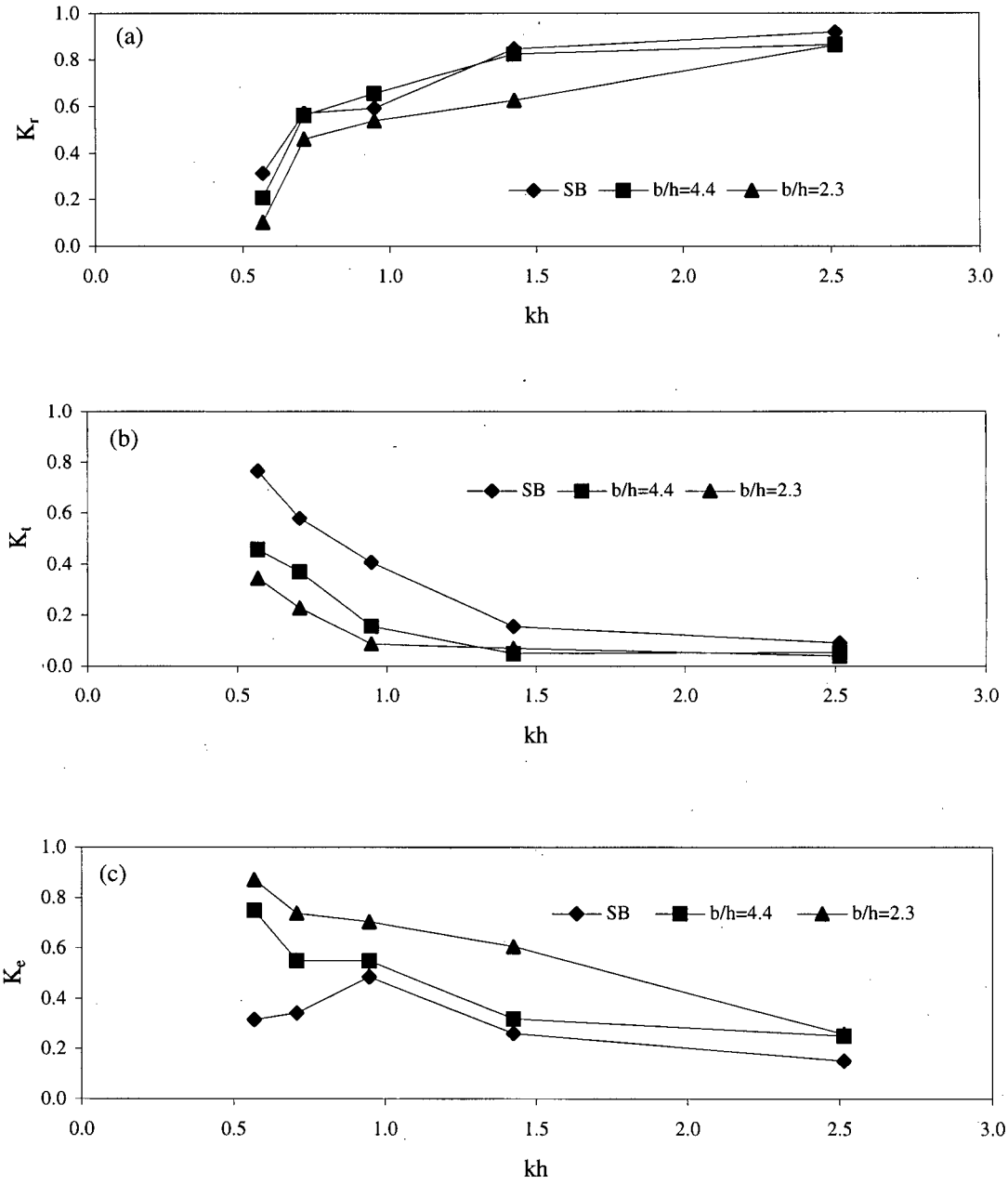

Figure 33. Comparison of hydrodynamic coefficients for single barrier (SB) and double barrier for a relative draft h/d = 0.5 and porosity ε = 0%. (a) reflection coefficient, (b) transmission coefficient, and (c) energy dissipation coefficient.

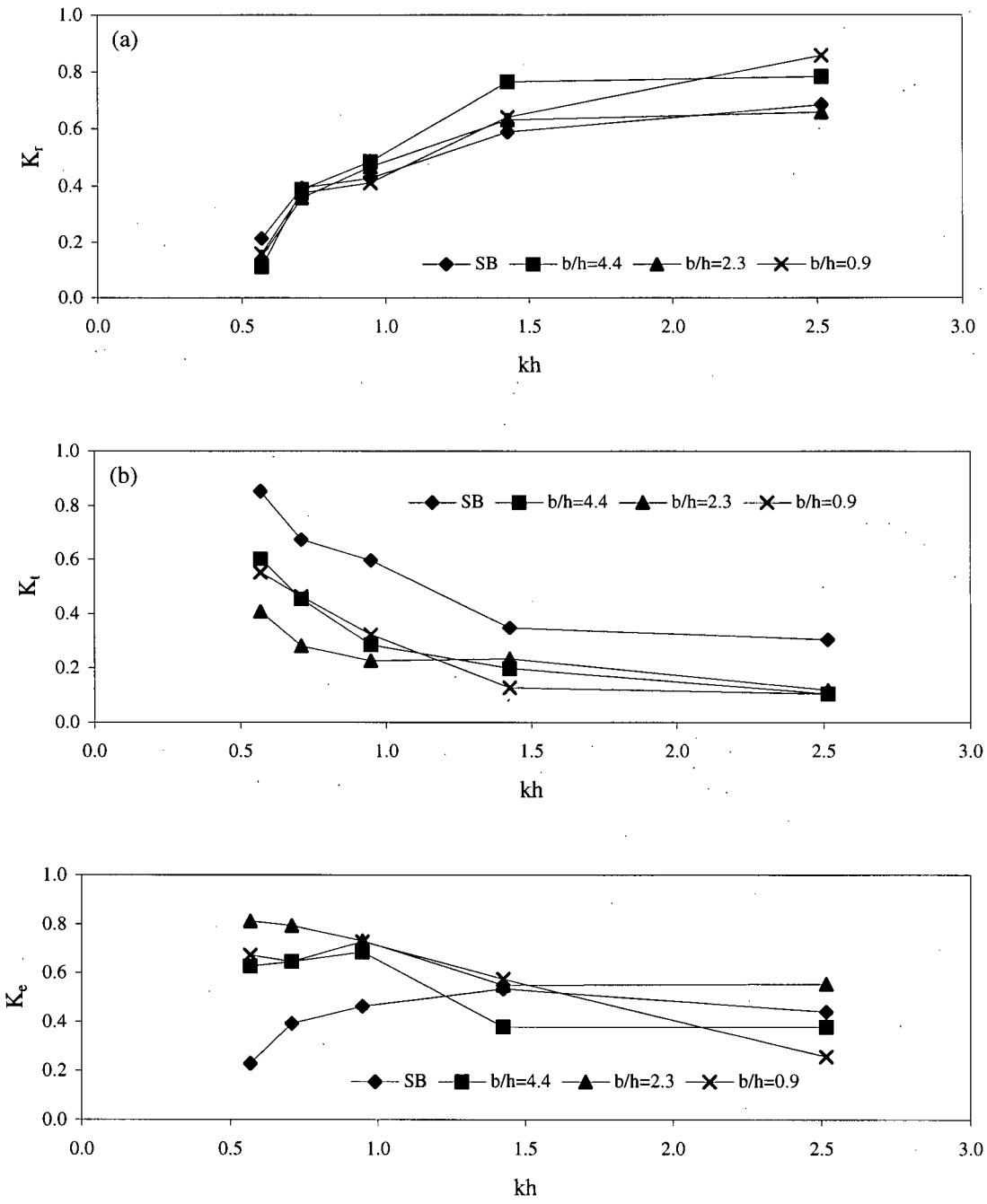

Figure 34. Comparison of hydrodynamic coefficients for single barrier and double barrier for a relative draft h/d = 0.5 and porosity ε = 5%. (a) reflection coefficient, (b) transmission coefficient, (c) energy dissipation coefficient.

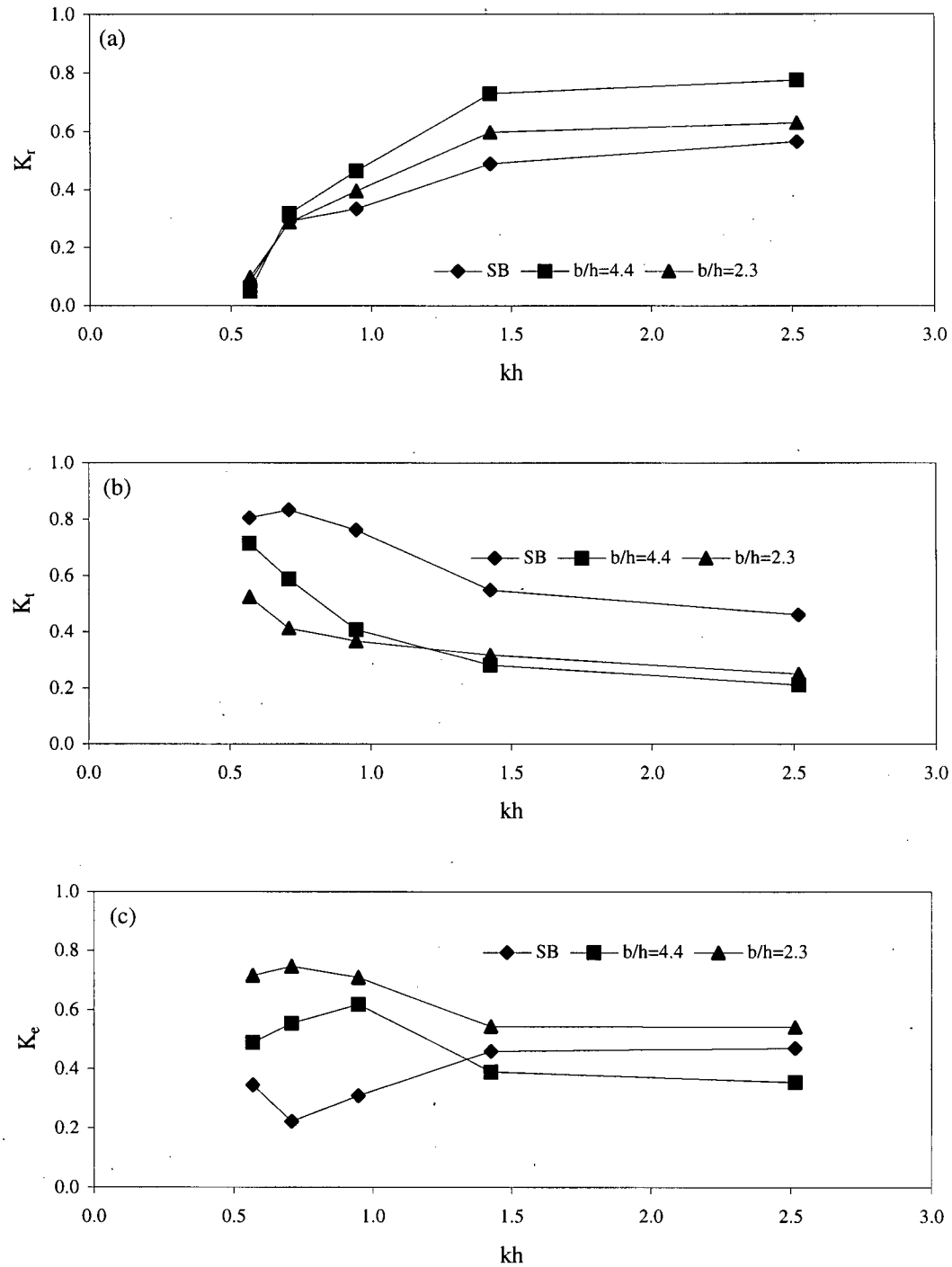

Figure 35. Comparison of hydrodynamic coefficients for single barrier and double barrier for a relative draft h/d = 0.5 and porosity ε = 10%. (a) reflection coefficient, (b) transmission coefficient, (c) energy dissipation coefficient.

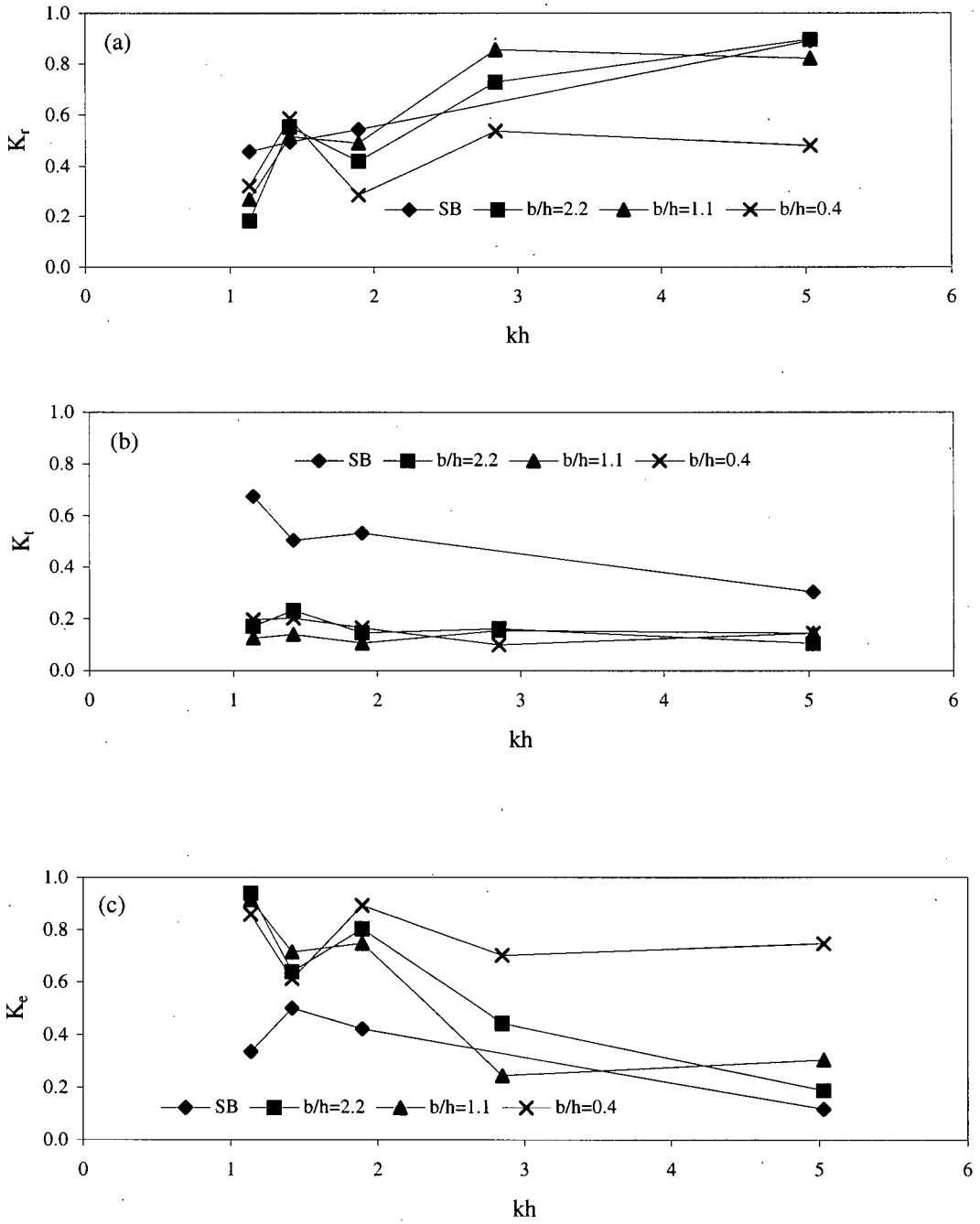

Figure 36. Comparison of hydrodynamic coefficients for single barrier and double barrier for a relative draft h/d = 1.0 and porosity ε = 5%. (a) reflection coefficient, (b) transmission coefficient, (c) energy dissipation coefficient.

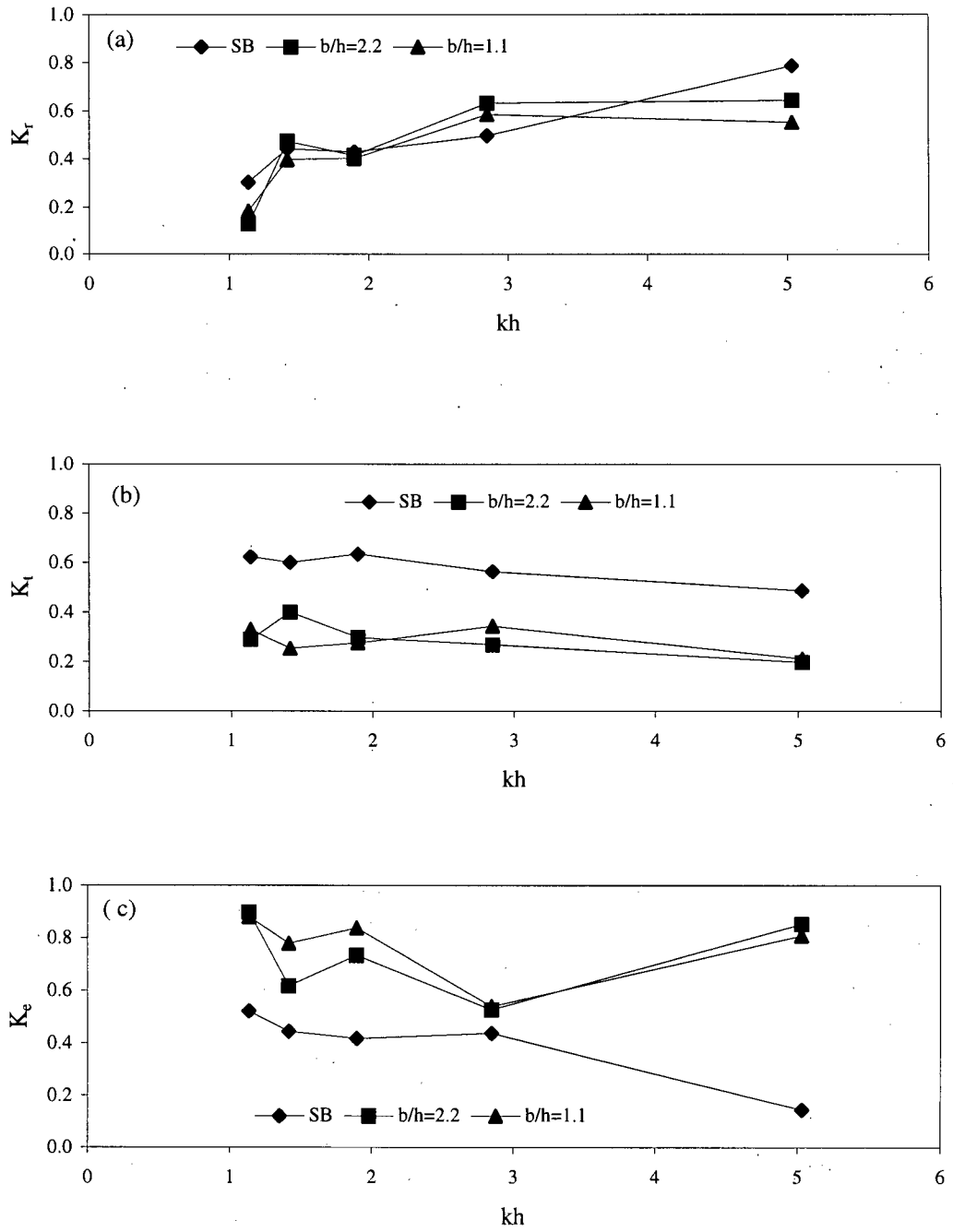

Figure 37. Comparison of hydrodynamic coefficients for single barrier and double barrier for a relative draft h/d = 1.0 and porosity ε = 10%. (a) reflection coefficient, (b) transmission coefficient, (c) energy dissipation coefficient.

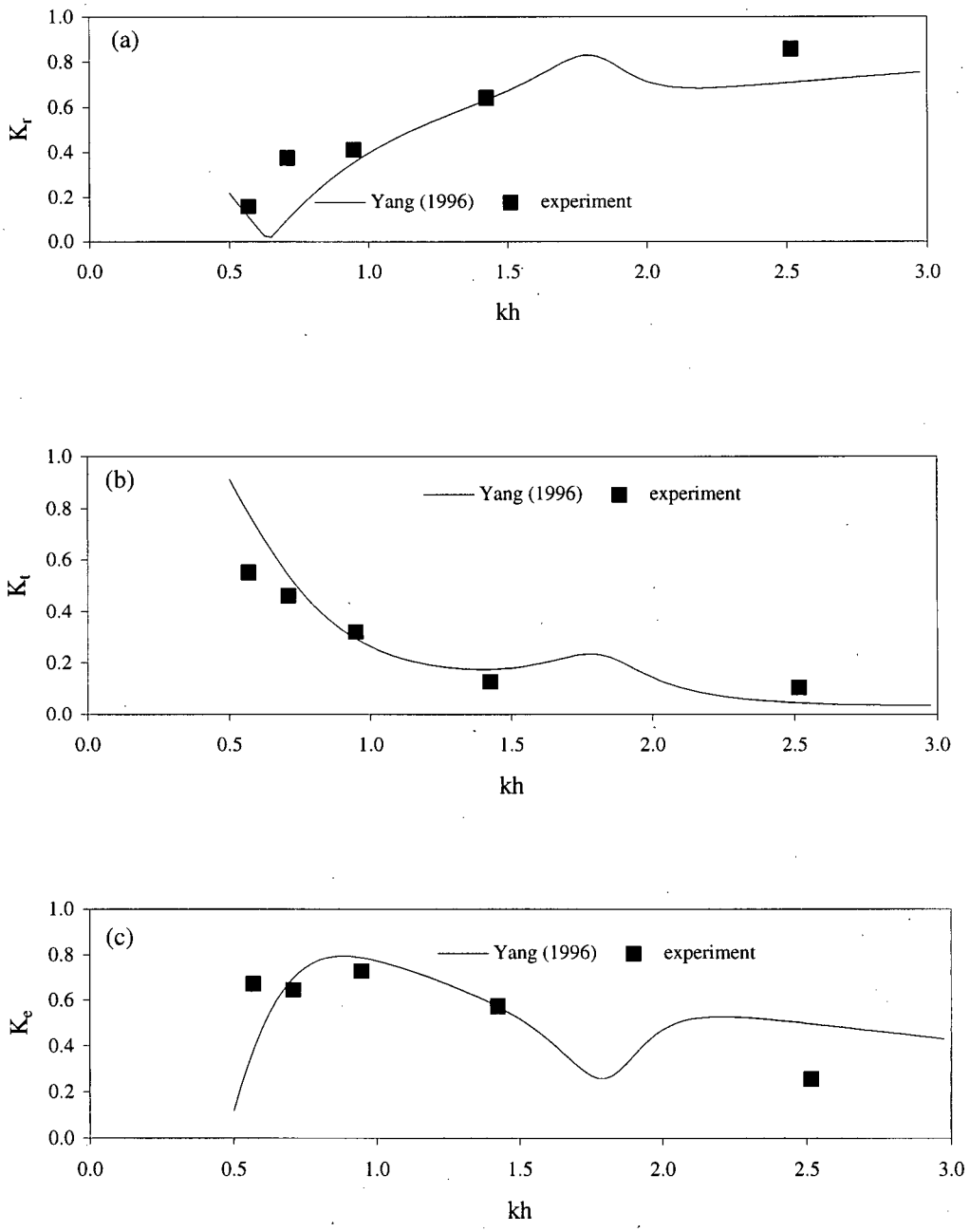

Figure 38. Comparison of experimental and numerical results for a double barrier as function of kh for a relative draft h/d = 0.5, relative distance b/h = 0.9 and porosity ε = 5%. (a) reflection coefficient, (b) transmission coefficient, (c) energy dissipation coefficient.

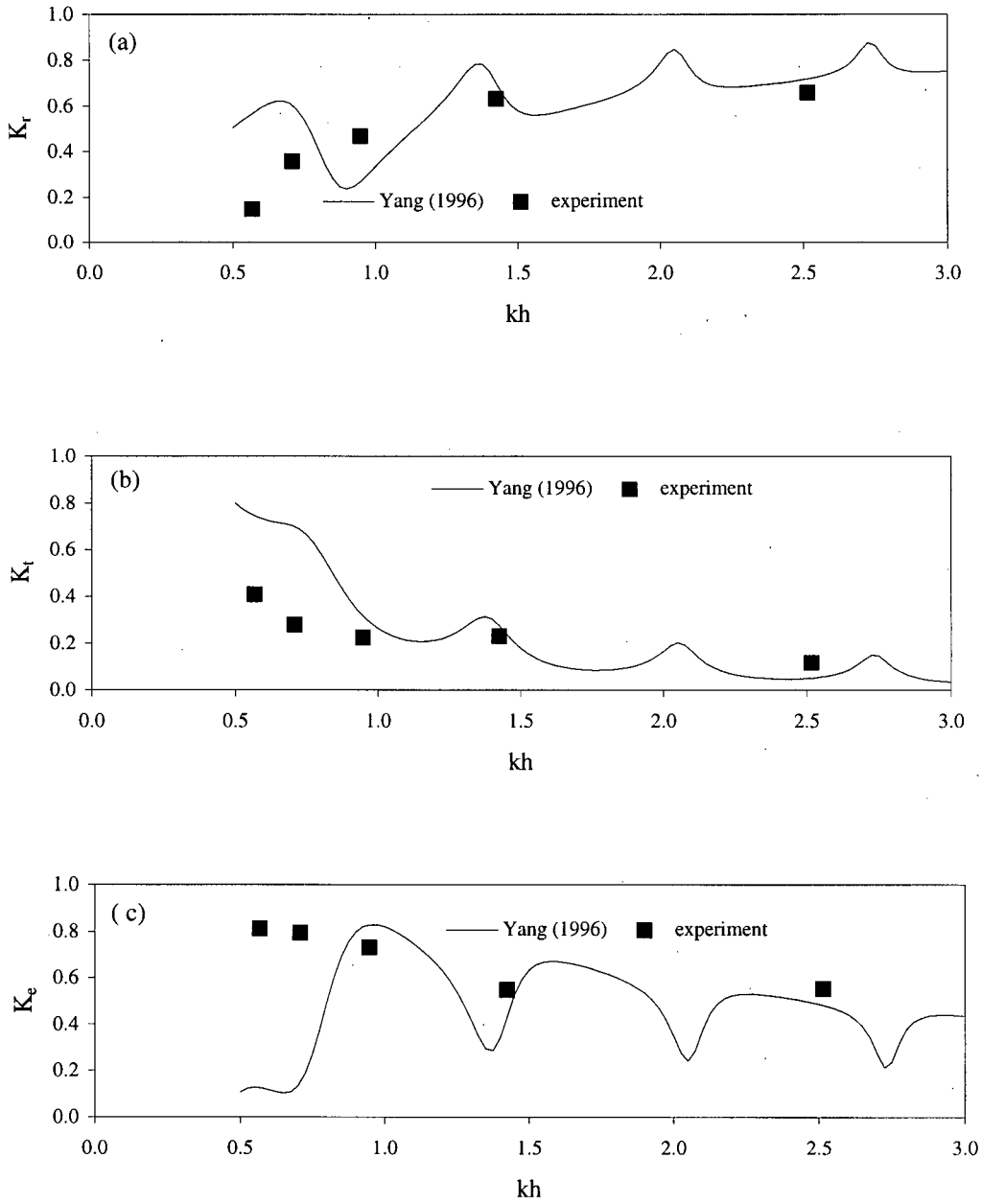

Figure 39. Comparison of experimental and numerical results for a double barrier as function of kh for a relative draft h/d = 0.5, relative distance b/h = 2.2 and porosity ε = 5%. (a) reflection coefficient, (b) transmission coefficient, (c) energy dissipation coefficient.

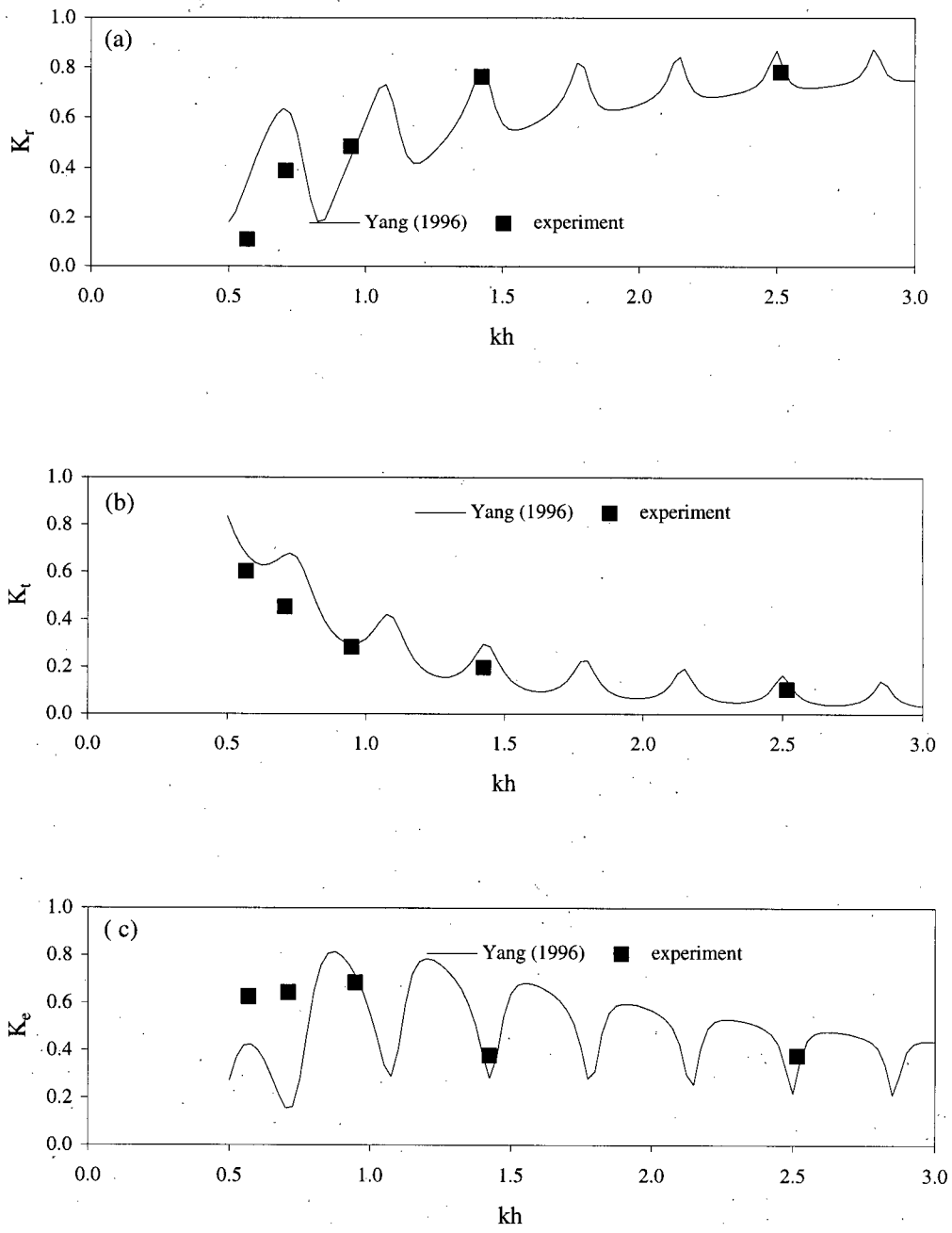

Figure 40. Comparison of experimental and numerical results for a double barrier as function of kh for a relative draft h/d = 0.5, relative distance b/h = 4.4 and porosity ε = 5%. (a) reflection coefficient, (b) transmission coefficient, (c) energy dissipation coefficient.